Electronic Supplementary Information

Highly Active Sulfur Based Pincer Ruthenium Catalyst for CO_2 Hydrogenation

Alexander Mondragón-Díaz,[a] Steven P. Kelley,[a] Nilay Hazari[b] and Wesley H. Bernskoetter[a,*]

[a]Department of Chemistry, University of Missouri, Columbia, MO USA. Email: bernskoetterwh@missouri.edu

[b]Department of Chemistry, Yale University, New Haven, CT USA.

Table of Contents

Synthetic Details and Selected Spectroscopy

General Procedures. All experiments were carried out under argon or dinitrogen atmospheres using standard Schlenk techniques in conjunction with an inert atmosphere glovebox under dinitrogen unless otherwise specified. All chemicals used in syntheses were purchased from Millepore Sigma, Fischer Scientific or Strem; isotopically enriched materials were purchased from Cambridge Isotope Laboratories. Solvents were dried using an MBraun-SPS system. 2-*tert*-butylsulfanyl bromobenzene was prepared according to literature procedures.[1] Unless otherwise noted below, reagents were commercially available and used as received. ^{1}H, ^{13}C{^{1}H}, and ^{31}P{^{1}H} NMR spectra were recorded on Bruker 300, 500, or 600 spectrometers in benzene-d_6, acetone-d_6, dichloromethane-d_2, acetonitrile-d_3, or THF-d_8 at ambient probe temperature (292 K). ^{1}H and ^{13}C NMR spectra were referenced to solvent signals,[2] while ^{31}P NMR spectra were referenced to an 85% phosphoric acid external standard. Elemental analysis (C, H, N) was conducted by Robertson Microlit Laboratories. IR characterization was conducted on pressed KBr pellets using a Nicolet Summit Pro FTIR spectrometer with iD1 transmission accessory. X-ray crystallography was conducted with a Bruker D8 Venture diffractometer equipped with a Photon II CMOS area detector using Mo-Kα radiation from a microfocus source. Samples were collected in inert oil and quickly transferred to a cold gas stream. The structures were solved from direct methods and Fourier syntheses and refined by full-matrix least-squares procedures with anisotropic thermal parameters for all non-hydrogen atoms.

[1] Harkins, S. B. and Peters, J. C. Amido-Bridged Cu_2N_2 Diamond Cores that Minimize Structural Reorganization and Facilitate Reversible Redox Behavior between a Cu^1Cu^1 and a Class III Delocalized $Cu^{1.5}Cu^{1.5}$Species. *J. Am. Chem. Soc.* **2004**, *126*, 2885-2893

[2] Fulmer, G. R.; Miller, A. J. M.; Sherden, N. H.; Gottlieb, H. E.; Nudelman, A.; Stoltz, B. M.; Bercaw, J. E.; Goldberg, K. I. NMR Chemical Shifts of Trace Impurities: Common Laboratory Solvents, Organics, and Gases in Deuterated Solvents Relevant to the Organometallic Chemist. *Organometallics* **2010**, *29*, 2176–2179. https://doi.org/10.1021/om100106e.

Synthesis of $CH_3P(C_6H_4S^tBu)_2$ ($^{tBu}SP^{Me}S$).

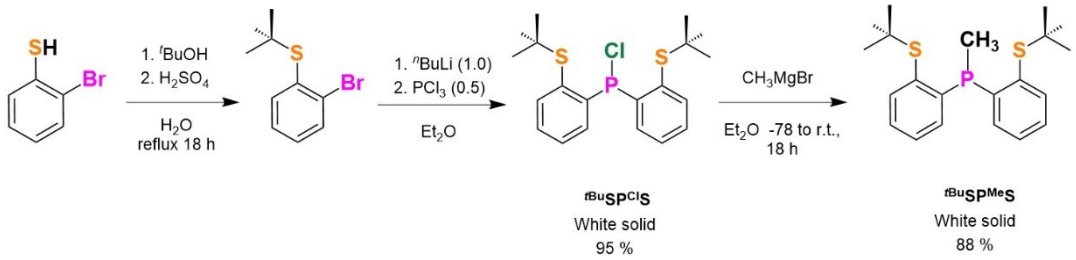

Scheme S1. Synthetic route to pincer ligand ($^{tBu}SP^{Me}S$).

Part A: *Synthesis of bis(2-(tert-butylthio)phenyl)chlorophosphine* ($^{tBu}SP^{Cl}S$). A solution of 2-*tert*-butylsulfanyl bromobenzene[1] (1.00 g, 4.08 mmol) in 15 mL of diethyl ether was frozen at -196 °C. The solid was layered with *n*-butyllithium (1.6 M solution in hexanes, 2.6 mL, 4.08 mmol), and the reaction was gradually warmed to room temperature. A white suspension was observed after 15 minutes of stirring. The reaction was allowed to continue for 2 h, then cooled to -78 ºC and transferred slowly (*ca* 30 min) using a cannula to a -78 ºC solution of PCl_3 (0.280 g, 2.04 mmol) in 5 mL of diethyl ether. The resulting suspension was allowed to warm to room temperature with continued stirring. The yellow reaction mixture slowly lost colour and after 2 h was filtered through Celite. The filtrate was collected. Removal of the volatiles afforded a light-yellow viscous oil that gradually solidified upon standing overnight to yield a nearly colourless solid (0.785 g, 97%). ^{1}H NMR (500 MHz, C_6D_6), δ 7.70 (d, J = 7.6 Hz, 2H, CH_{Ar}), 7.47 – 7.37 (m, 2H, CH_{Ar}), 6.96 (dtd, J = 20.9, 7.4, 1.6 Hz, 4H, CH_{Ar}), 1.32 (s, 18H, S$(CH_3)_3$). ^{13}C{^{1}H} NMR (126 MHz, C_6D_6) δ 148.23 (d, J_{PC} = 32.7 Hz, 2C, C_{Ar}), 137.96 (s, 2C, C_{Ar}), 136.90 (d, J_{PC} = 34.5 Hz, 2C, C_{Ar}), 133.09, 129.74, 129.55 (d, $^2J_{PC}$ = 1.0 Hz), 48.53, 31.33 (d, $^2J_{PC}$ = 2.7 Hz).^{31}P{^{1}H} (202 MHz, C_6D_6): δ 56.24.

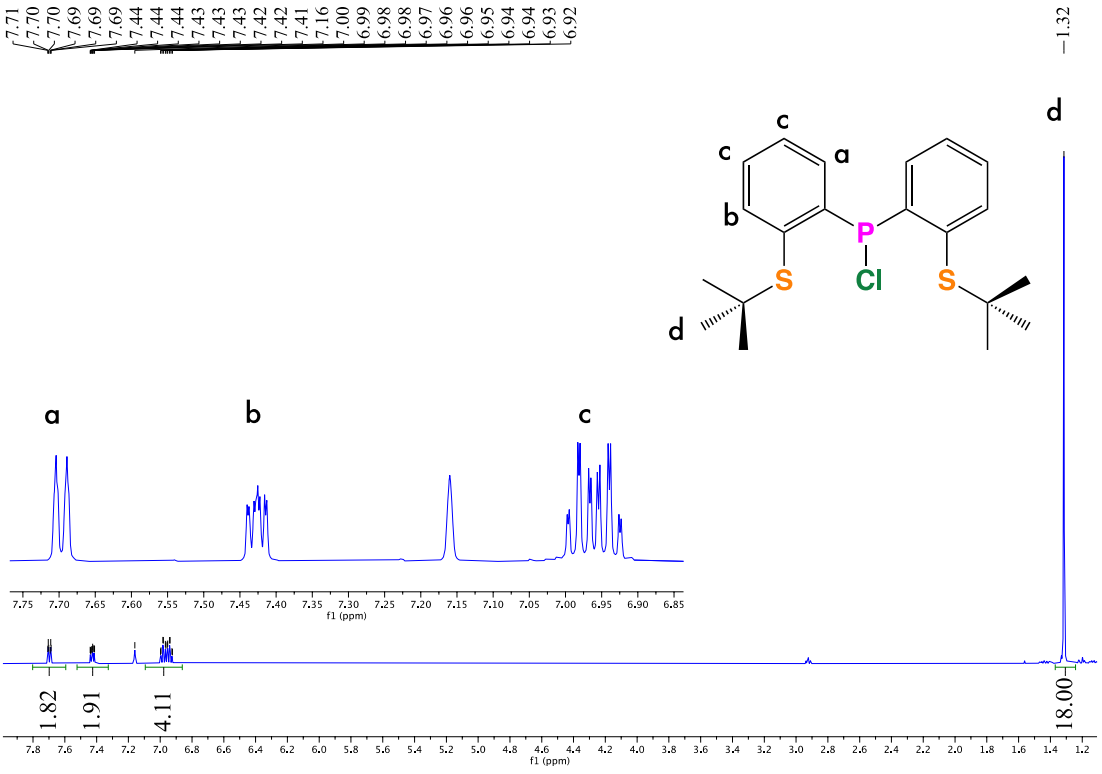

Figure S1. ^{1}H NMR (500 MHz) spectrum of ^{tBu}**SP**^{Cl}**S** in C_6D_6.

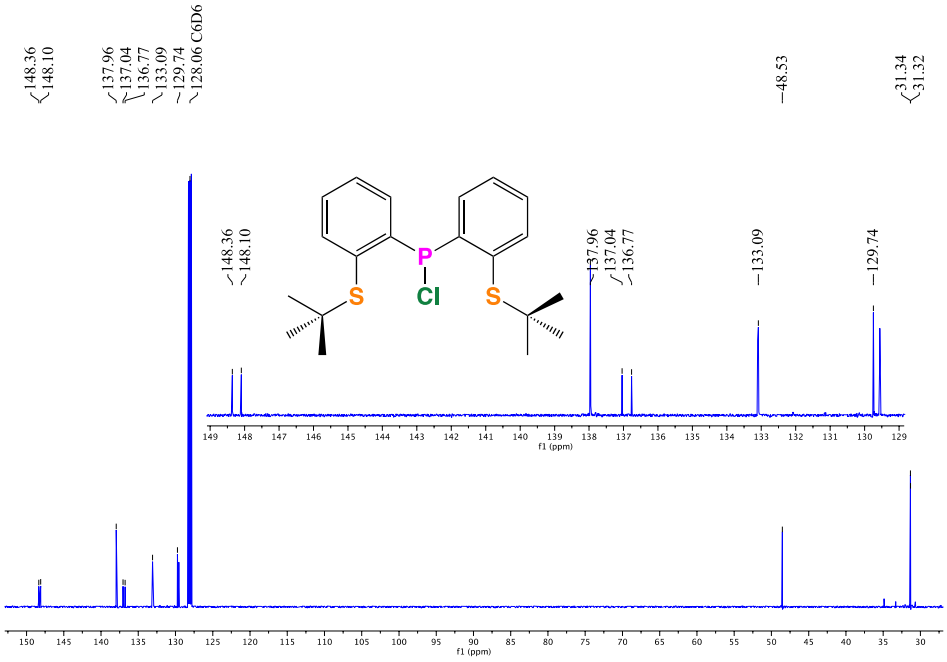

Figure S2. ^{13}C{^{1}H} NMR (126 MHz) spectrum of ^{tBu}**SP**^{Cl}**S** in C_6D_6.

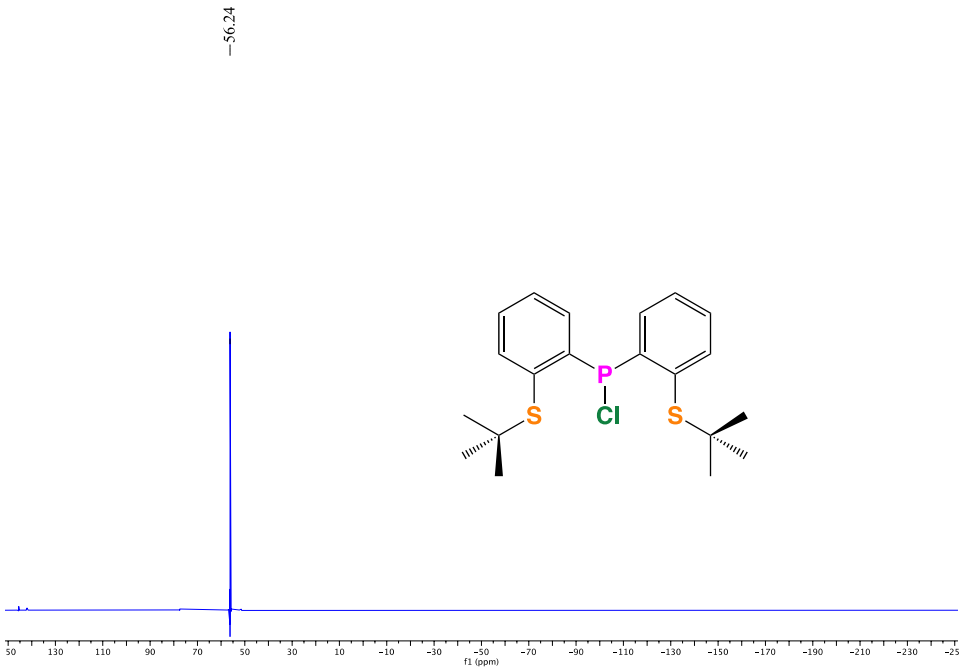

Figure S3. $^{31}P\{^{1}H\}$ (202 MHz) spectrum of $^{tBu}SP^{Cl}S$ in C_6D_6.

Part B: *Synthesis of bis(2-(tert-butylthio)phenyl)(methyl)phosphine*. A suspension of $^{tBu}SP^{Cl}S$ (0.600 g, 1.510 mmol) in 15 mL of diethyl ether was chilled to –78 °C and treated dropwise with a MeMgBr solution (0.503 mL, 3.0 M in Et_2O, 1.51 mmol). The reaction mixture was gradually warmed to room temperature and stirred for an additional 4 hours. The resulting solution was concentrated under reduced pressure until the precipitation of magnesium salts was observed. The mixture was then filtered, and the solid residue was washed sequentially with diethyl ether (3 × 5 mL) and dichloromethane (2 × 5 mL). The combined filtrates were passed through a Celite pad to ensure complete removal of any residual salts. All volatiles were removed under reduced pressure and $^{tBu}SP^{Me}S$ (0.500 g, 87.9%) isolated as a colorless solid without further purification. ^{1}H NMR (500 MHz, C_6D_6, ppm) δ 7.68 – 7.58 (m, 2H, CH_{Ar}), 7.08 – 7.04 (m, 2H, CH_{Ar}), 6.99 (tdd, J = 7.3, 1.8 Hz, 4H, CH_{Ar}), 1.54 (d, J_{PC} = 6.4 Hz, PCH_3, 3H), 1.40 (s, 18H, S$(CH_3)_3$). $^{13}C\{^{1}H\}$ NMR (126 MHz, C_6D_6, ppm) δ 149.49 (d, J = 13.8 Hz, 2C), 138.76 (d, J = 1.3 Hz, 2C), 138.00 (s, 2C), 137.80 (s, 2C), 131.89 (s, 2C), 129.25 (s, 2C), 48.16 (s, 2C), 31.49 (d, J = 4.5 Hz), 12.77 (d, J = 18.1 Hz, PCH_3). $^{31}P\{^{1}H\}$ NMR (202 MHz, C_6D_6, ppm) δ –34.3 (s).

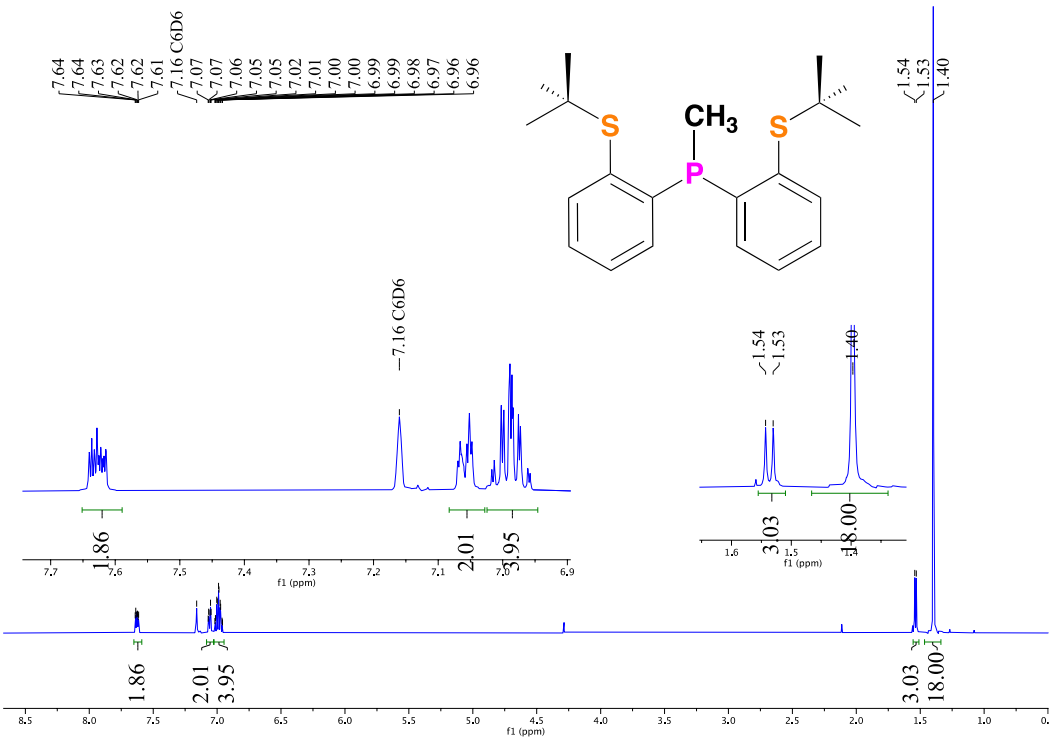

Figure S4. ^{1}H NMR (500 MHz) spectrum of **^{tBu}SP^{Me}S** in C_6D_6.

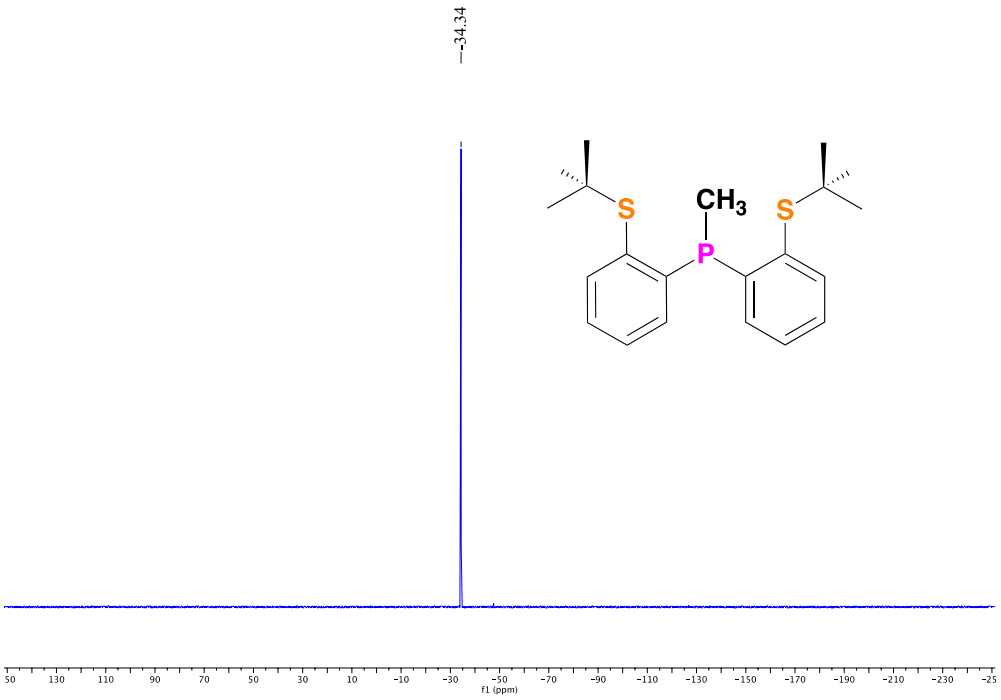

Figure S5. ^{31}P{^{1}H} (202 MHz) spectrum of **^{tBu}SP^{Me}S** in C_6D_6.

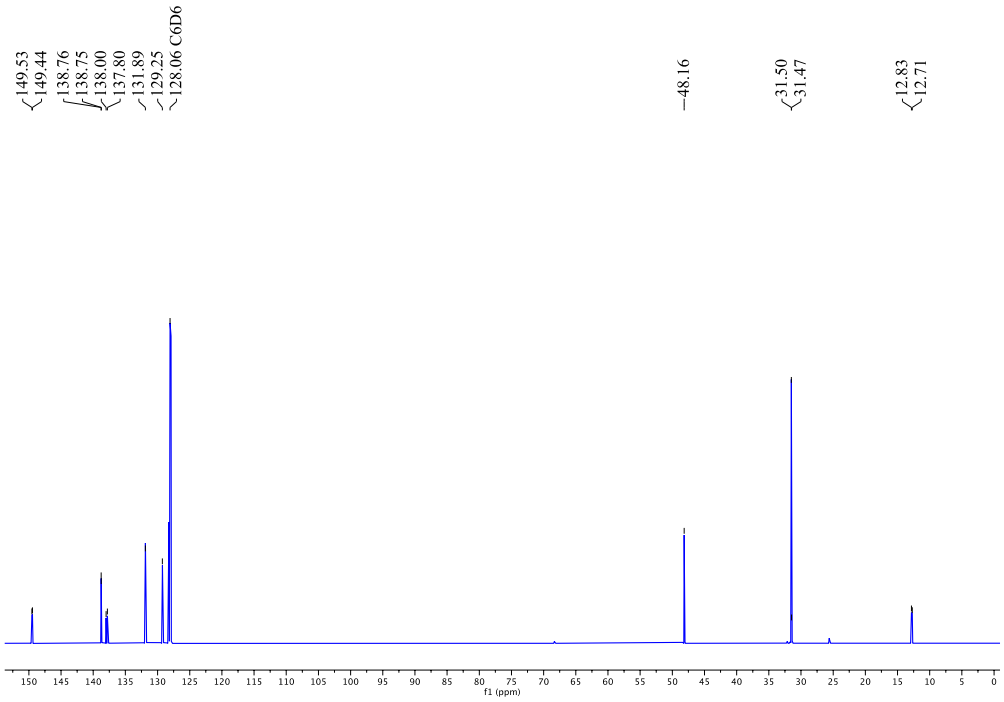

Figure S6. $^{13}C\{^{1}H\}$ NMR (126 MHz) spectrum of **^{tBu}SP^{Me}S** in C_6D_6.

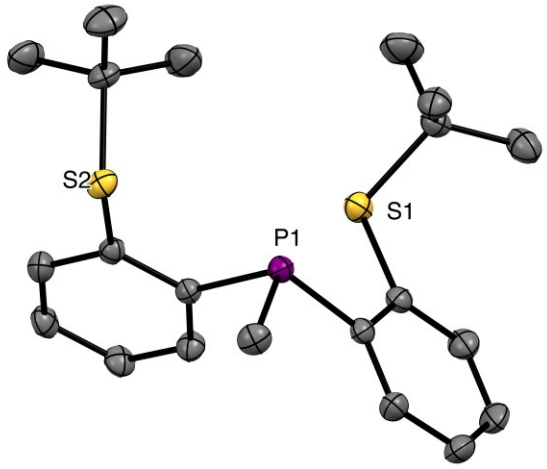

Figure S7. Molecular structure of **^{tBu}SP^{Me}S**. Ellipsoids at 50% probability level. Hydrogen atoms are omitted for clarity. Color code: C, gray; S, yellow; P, purple. (XRD quality crystals were obtained from a concentrated solution of THF at -42 ºC).

Preparation of Ru(κ^3-^{tBu}SP^{Me}S)(PPh$_3$)Cl$_2$ (1-Cl$_2$). A 250 mL Schlenk flask containing a mixture of $Ru(PPh_3)_3Cl_2$ (0.341 g, 0.355 mmol) and **^{tBu}SP^{Me}S** (0.134 g, 0.355 mmol) in 50 mL of toluene was stirred at room temperature for 1 h producing a yellow suspension. The

product was collected by filtration, washed with diethyl ether (2 x 10 mL), pentane (2 x 10 mL) and dried under vacuum to yield 0.273 g of **1-Cl$_2$** as a yellow solid (95 %).^{1}H NMR (500 MHz, CD_2Cl_2) δ 7.81 (dt, *J* = 5.7, 2.9 Hz, 1H, C*H*$_{Ar}$), 7.68 (t, *J* = 7.5 Hz, 1H, C*H*$_{Ar}$), 7.61 (br, 6H, C*H*$_{Ar}$), 7.48 (t, *J* = 7.5 Hz, 1H, C*H*$_{Ar}$), 7.34 (br, 1H, C*H*$_{Ar}$), 7.35 – 7.29 (m, 2H, C*H*$_{Ar}$), 7.26 (t, *J* = 6.6 Hz, 3H, C*H*$_{Ar}$), 7.21 (d, *J* = 7.6 Hz, 1H, C*H*$_{Ar}$), 7.14 (t, *J* = 7.8 Hz, 6H, C*H*$_{Ar}$), 6.85 (d, *J* = 7.8 Hz, 1H, C*H*$_{Ar}$), 1.75 (s, 9H, S*(CH$_3$)$_3$*), 0.90 (s, 9H, S*(CH$_3$)$_3$*), 0.82 (d, *J* = 10.5 Hz, 3H, P*CH$_3$*). ^{13}C{^{1}H} NMR (126 MHz, $CDCl_3$), δ 146.40 (d, *J* = 2.2 Hz), 146.08 (d, *J* = 2.3 Hz), 144.95, 144.64, 144.39 (d, *J* = 23.3 Hz), 141.19 (dd, *J* = 22.9, 2.1 Hz), 135.62 (d, *J* = 8.2 Hz), 134.60 (d, *J* = 42.4 Hz), 133.87 (d, *J* = 19.3 Hz), 131.98 (dd, *J* = 10.7, 2.5 Hz), 131.33 (d, *J* = 11.0 Hz), 130.32 (d, *J* = 35.1 Hz), 129.48 (dd, *J* = 31.1, 1.8 Hz), 128.91 (d, *J* = 5.4 Hz), 128.67 (d, *J* = 2.6 Hz), 126.91 (d, *J* = 9.3 Hz), 60.12, 56.58 (d, *J* = 3.4 Hz), 31.99, 30.87, 6.23 (d, *J* = 30.2 Hz). ^{31}P{^{1}H} NMR (202 MHz, CD_2Cl_2) δ 86.72 (d, SPS, *J* = 26.3 Hz. S*P*S), 28.55 (d, *J* = 24.4 Hz, *P*Ph$_3$).

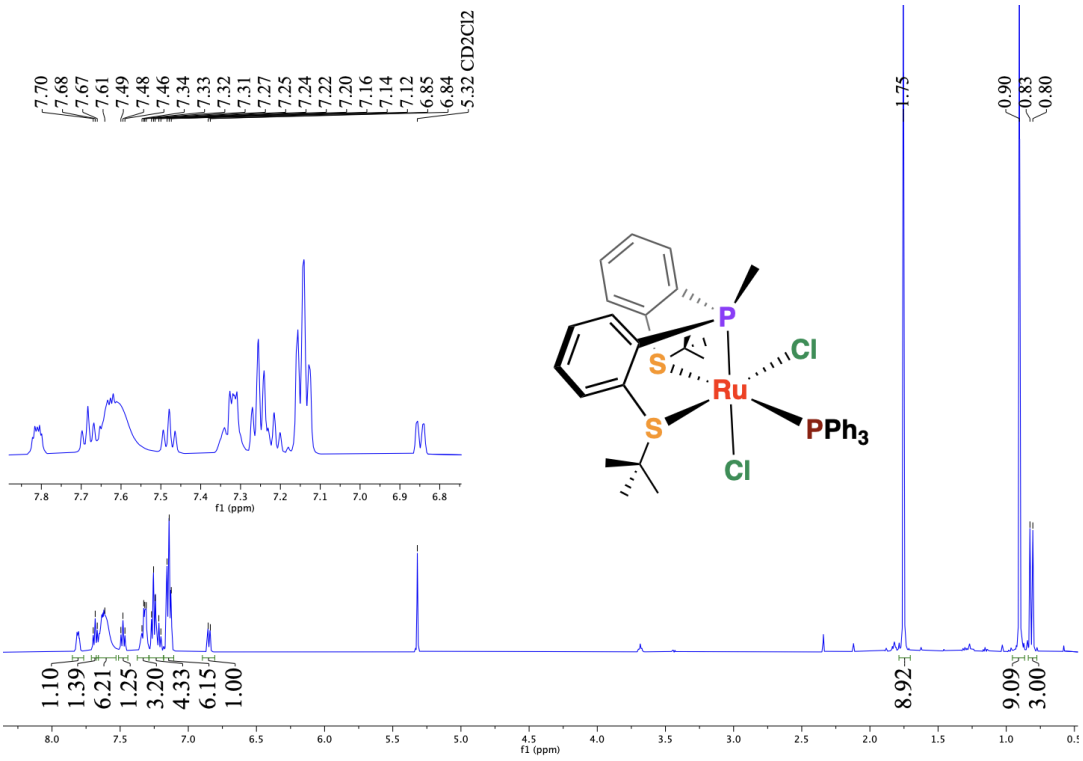

Figure S8. ^{1}H NMR (500 MHz) spectrum of **1-Cl$_2$** in CD_2Cl_2.

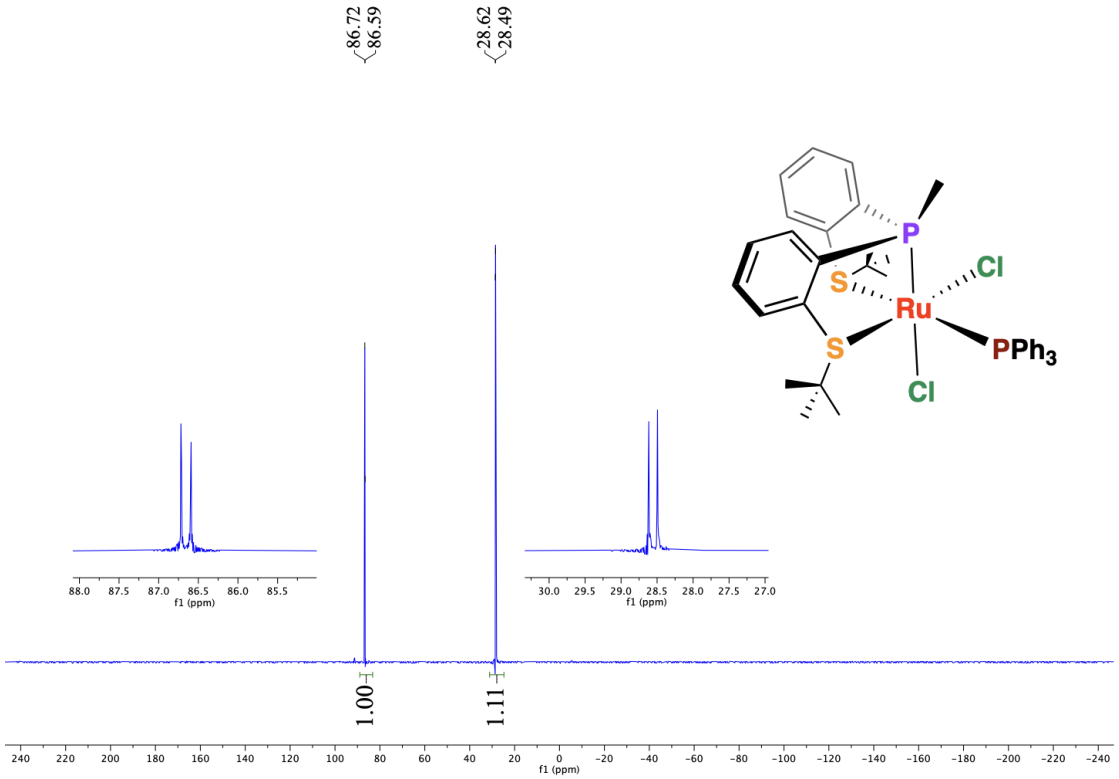

Figure S9. $^{31}P\{^{1}H\}$ (202 MHz) spectrum of **1-Cl₂** in CD_2Cl_2.

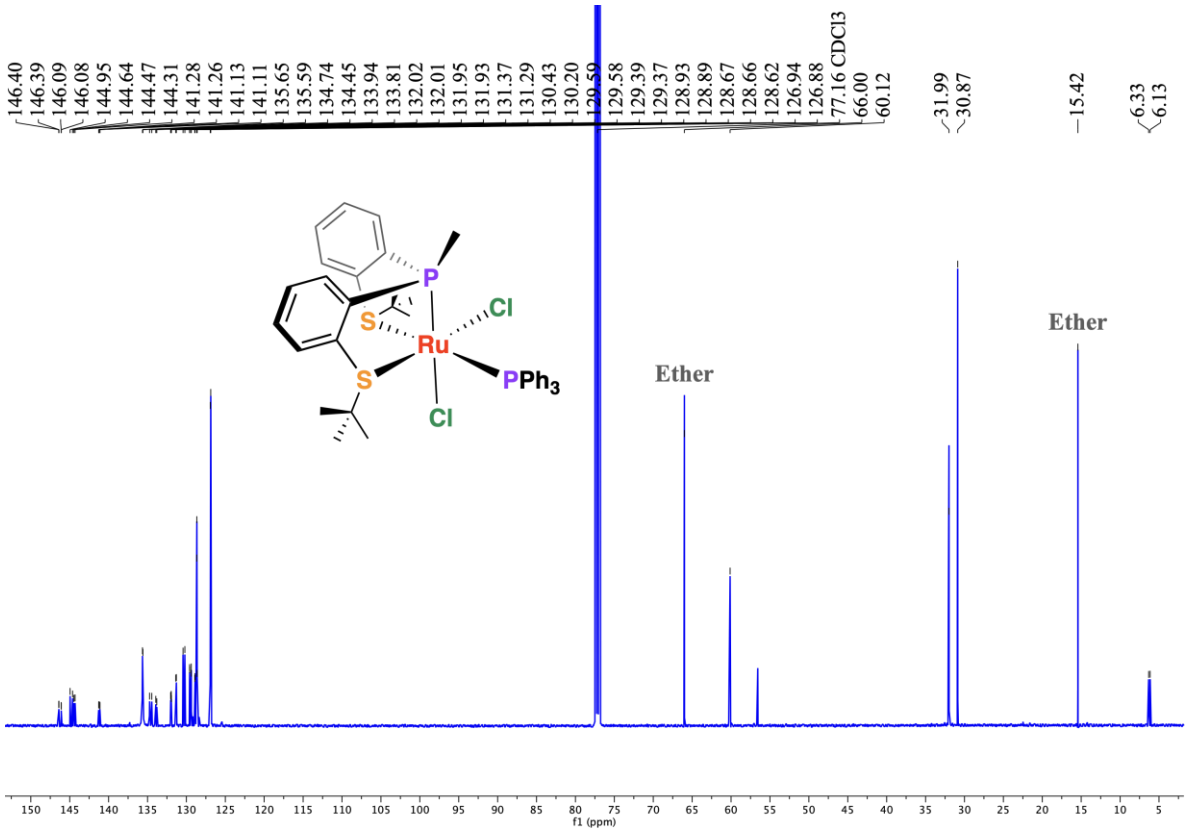

Figure S10. $^{13}C\{^{1}H\}$ (126 MHz) spectrum of **1-Cl₂** in $CDCl_3$.

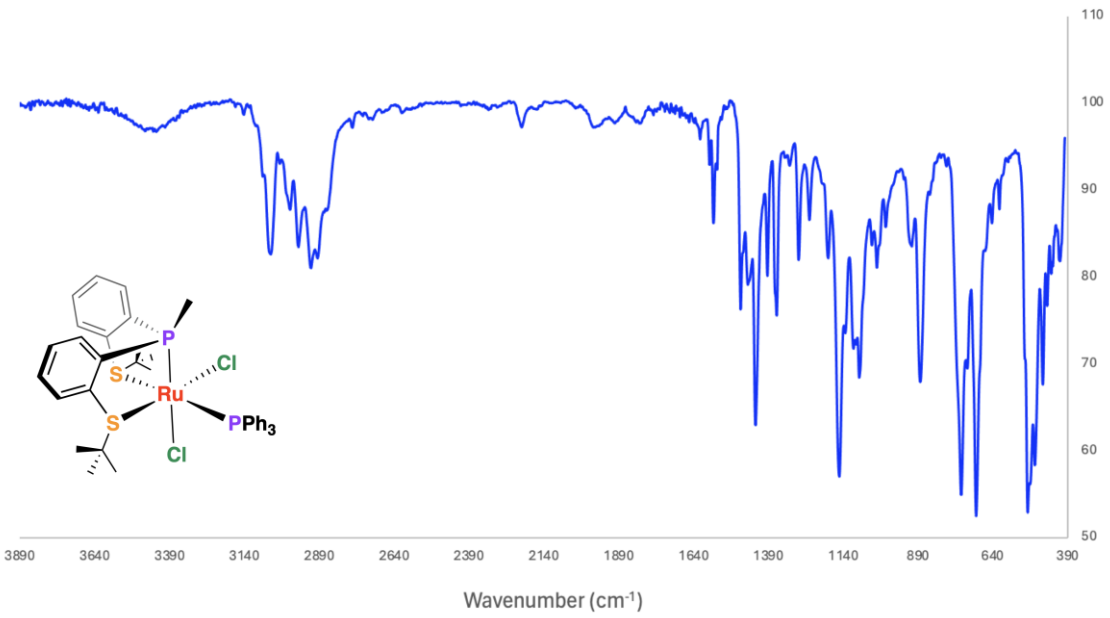

Figure S11. Solid-state IR spectrum of **1-Cl$_2$** in KBr.

Preparation of Ru(H)$_2$(κ^3-S^{tBu}P^{Me}S^{tBu})(PPh$_3$) (1-H$_2$). In a 250 mL Schlenk flask, a bright-yellow suspension of **1-Cl$_2$** (150 mg, 0.185 mmol) in 100 mL of dry ethanol was treated with $NaBH_4$ (70 mg, 1.85 mmol) in one portion with vigorous stirring. Gas evolution was immediately observed, and the bright-yellow suspension changed to a deep lime solution. After stirring at ambient temperature for 4 h, the reaction mixture was placed under vacuum and the volatiles removed. The solid residue was reconstituted in 50 mL of toluene, filtered through a fine frit and the filtrate treated with NEt_3 (2.0 equiv). The solution was stirred for 3 h, then concentrated under vacuum and layered with pentane. Cooling this mixture to -42 °C overnight afforded 124 mg (90 %) of **1-H$_2$** as yellow crystalline solid. Solutions of **1-H$_2$** in benzene solvent do not immediately degrade in air, but small changes to the NMR spectra of samples occur over 4-6 hours, thus **1-H$_2$** was stored and used under inert atmosphere. ^{1}H NMR (600 MHz, C_6D_6) δ 7.95 (t, J = 6.7 Hz, 6H, CH_{Ar}), 7.63 (d, J = 7.8 Hz, 1H, CH_{Ar}), 7.61 – 7.57 (m, 1H, CH_{Ar}), 7.49 – 7.44 (m, 1H, CH_{Ar}), 7.22 (d, J = 7.9 Hz, 1H, CH_{Ar}), 7.07-6.93 (m, 10H, CH_{Ar}), 6.88 (t, J = 5.6 Hz, 1H, CH_{Ar}), 6.81 (t, J = 6.2 Hz, 1H, CH_{Ar}), 6.75 (t, J = 7.5 Hz, 1H, CH_{Ar}), 1.60 (s, 9H, S$(CH_3)_3$), 1.26 (d, $^2J_{PH}$ = 5.1 Hz, 3H, PCH_3), 1.10 (s, 9H, S$(CH_3)_3$), -5.05 (ddd, J = 102.2, 28.1, 7.1 Hz, 1H, RH), -12.04 (ddd, J = 30.9, 14.8, 7.0 Hz, 1H, RH). ^{13}C{^{1}H} NMR (151 MHz, C_6D_6) δ 145.86 (d, J = 5.0 Hz), 145.68, 145.49, 145.28

(d, J = 9.5 Hz), 145.12, 143.99, 143.72, 142.38 (d, J = 2.7 Hz), 142.14, 134.38 (d, J = 11.0 Hz), 132.89 (d, J = 10.7 Hz), 132.6 (dd, J = 34.5, 5 Hz), 129.69, 129.12, 128.35, 127.34 (d, J = 8.8 Hz), 52.38, 51.10 (d, J = 5.0 Hz), 31.56, 29.97, 14.22 (d, J = 12.5 Hz). $^{31}P\{^{1}H\}$ NMR (202 MHz, C_6D_6) δ 76.22 – 75.09 (m, 1P, S*P*S), 73.50 (dd, J = 12.2, 5.6 Hz, PPh_3). IR, solid state (cm^{-1}): 1935 (Ru-H), 1720 (Ru-H) Anal. Calcd for $C_{39}H_{46}P_2RuS_2$: C, 63.12; H, 6.25. Found: C, 63.51; H, 5.94.

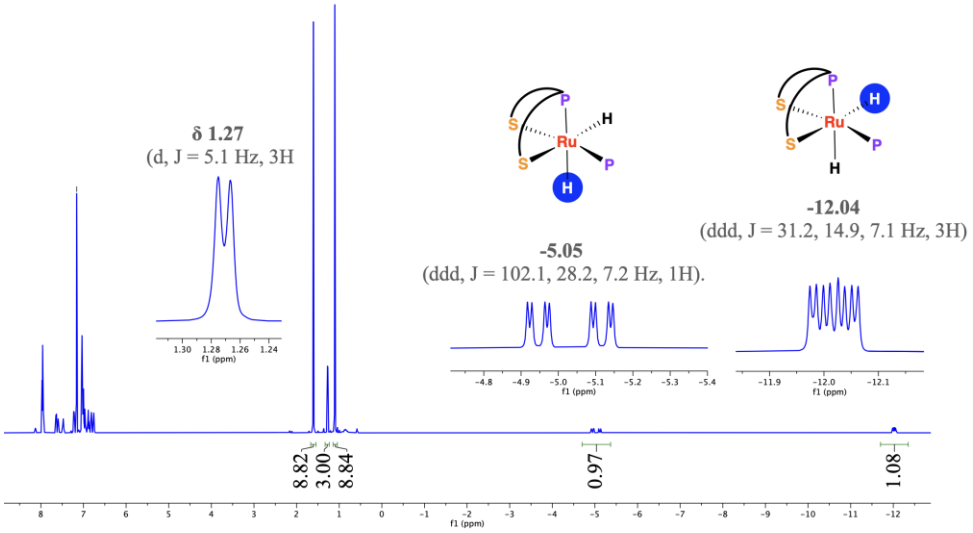

Figure S12. ^{1}H NMR (500 MHz) spectrum of **1-H₂** in C_6D_6.

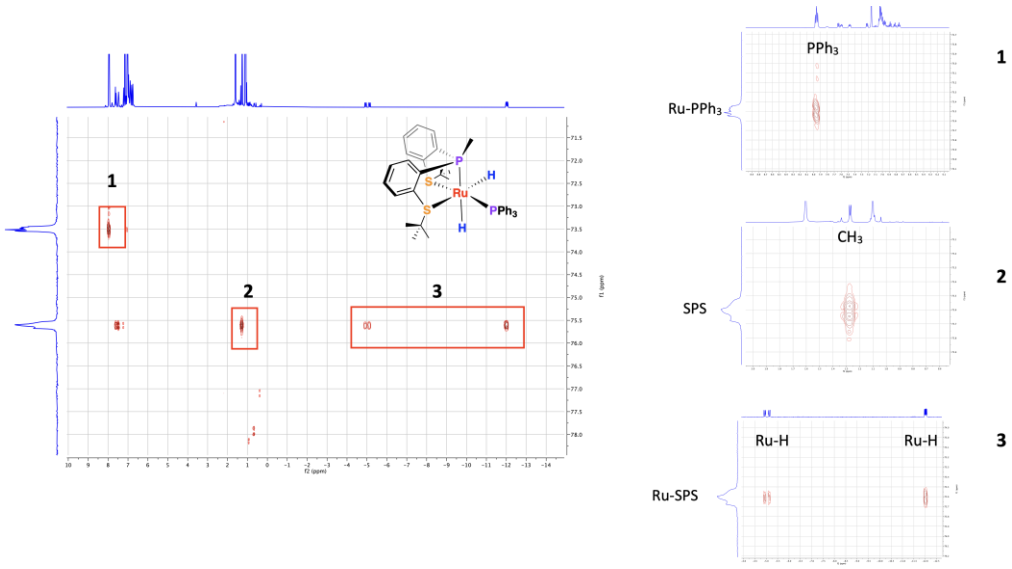

Figure S13. ^{1}H-^{31}P HMBC NMR of **1-H₂** in C_6D_6 (left) and an inset (right) showing a correlation between the phosphorus atoms from PPh_3 and SPS ligand with the aromatic protons (**1**) and methyl substituent (**2**) respectively. A correlation between the hydride ligand and the phosphorus atom from the SPS ligand (**3**) is also evident.

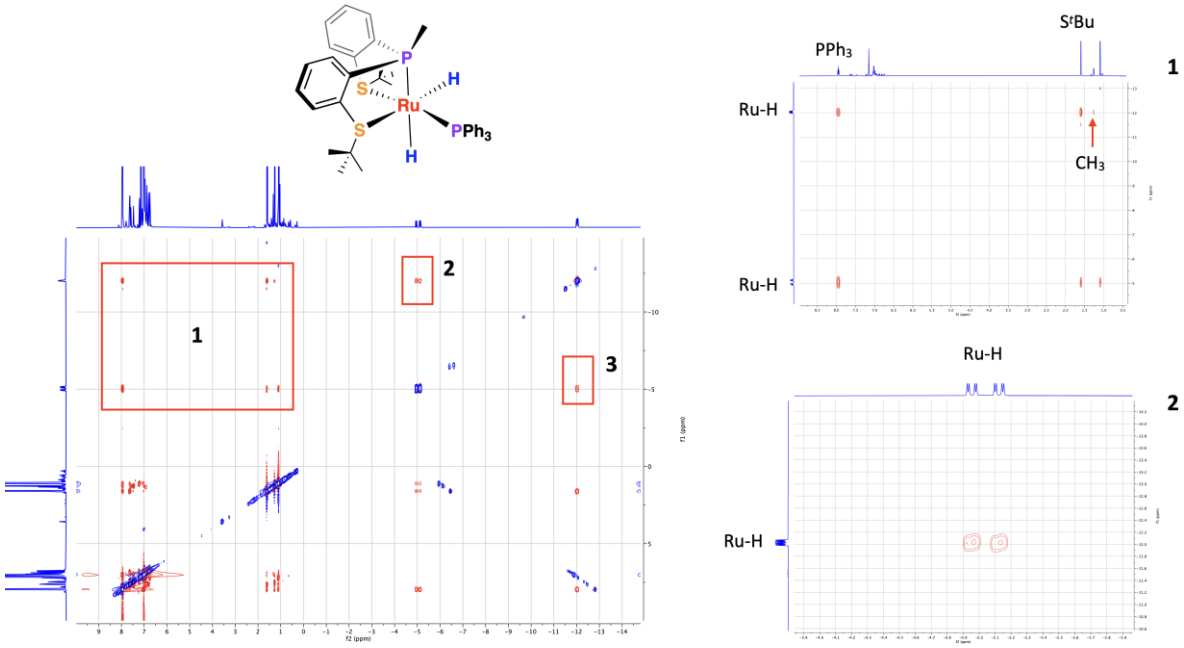

Figure S14. ^{1}H NOESY NMR of **1-H$_2$** in C_6D_6 (left) and an inset (right) showing an NOE correlation between the hydride ligands and the aromatic protons from PPh_3 and $P(CH_3)$ (**1**) and between the hydride ligands (**2** & **3**).

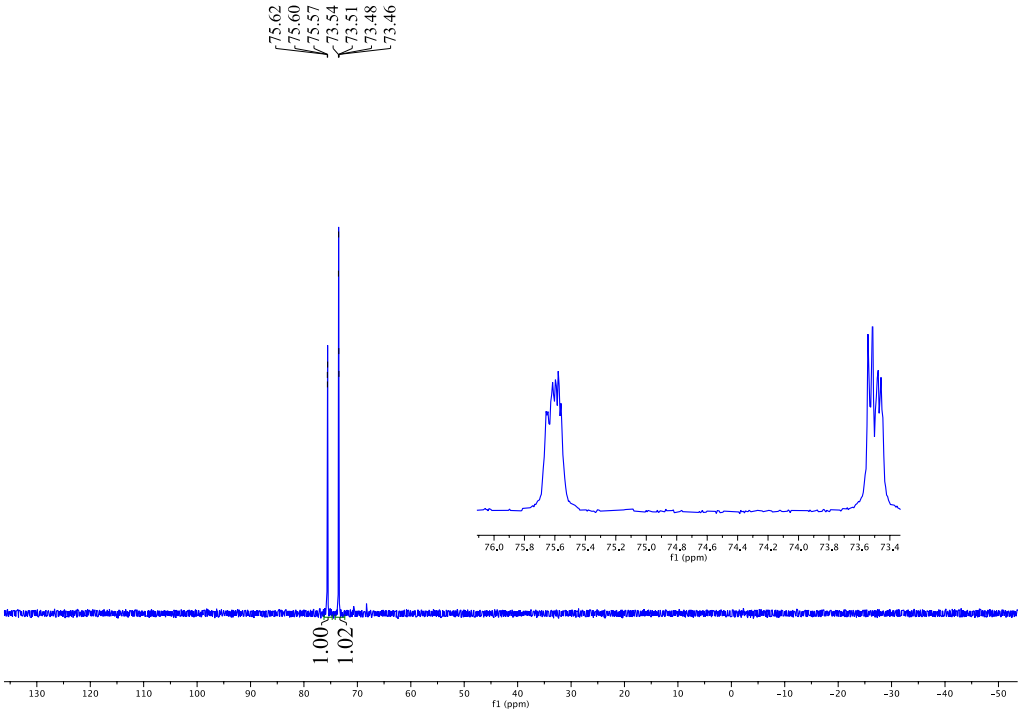

Figure S15. ^{31}P{^{1}H} NMR (202 MHz) spectrum of **1-H$_2$** in C_6D_6. Some ^{31}P-^{1}H coupling from Ru-H resonances was incompletely decoupled.

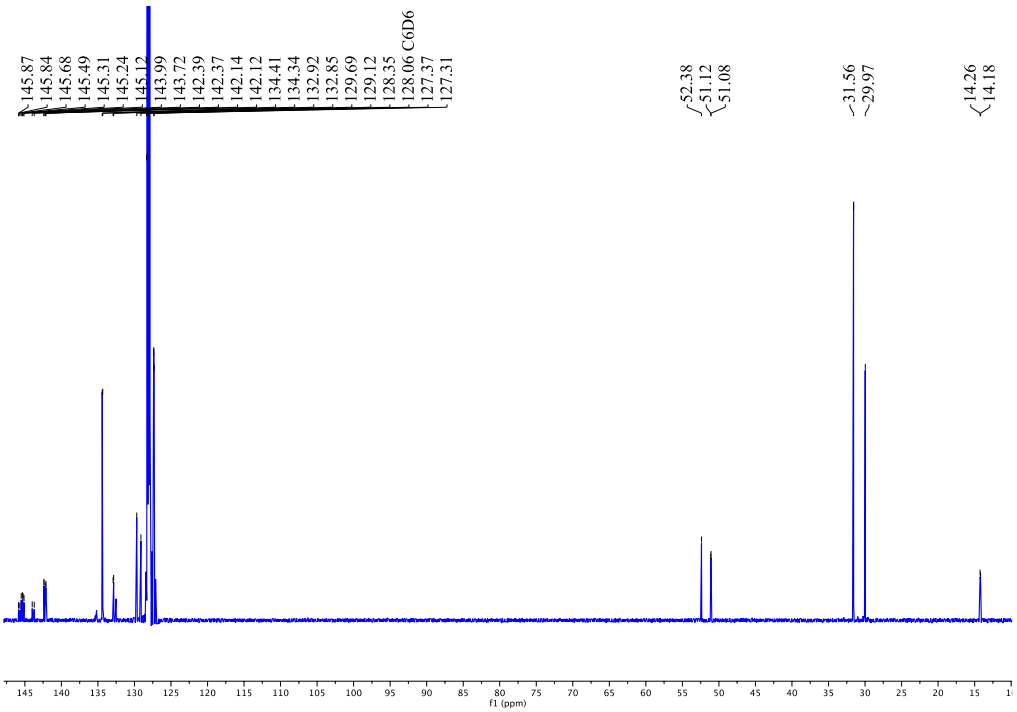

Figure S16. $^{13}C\{^{1}H\}$ NMR (126 MHz) spectrum of **1-H₂** in C_6D_6.

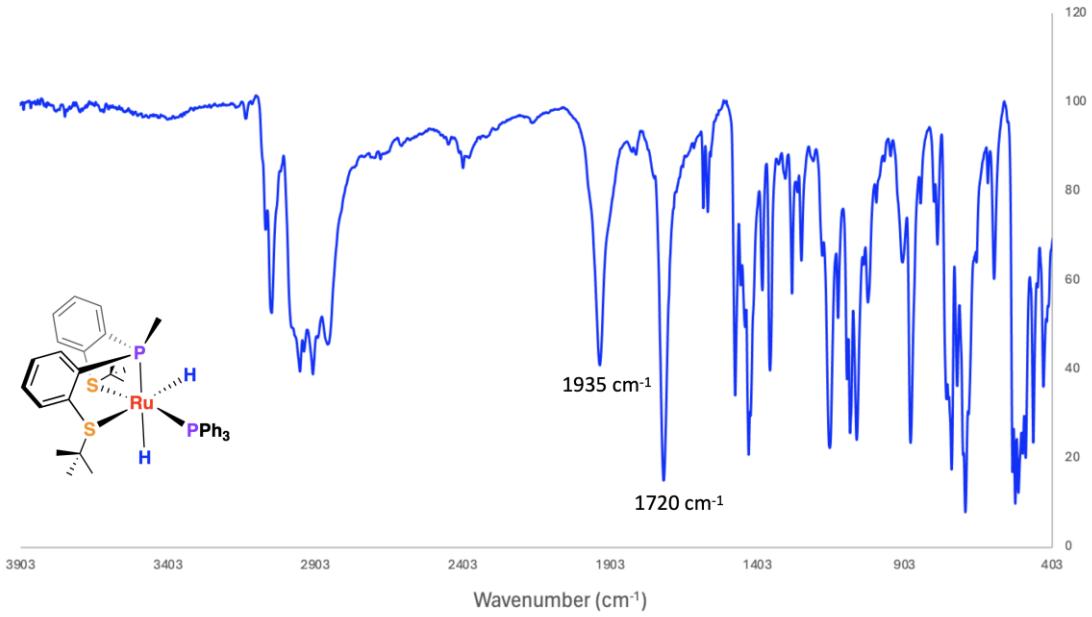

Figure S17. Solid-state IR spectrum of **1-H₂** in KBr.

Observation and Characterization of Ru(H)(BH_4)(κ^3-$S^{tBu}P^{Me}S^{tBu}$)(PPh_3) (1-BH_4). A 20 mL scintillation vial equipped with a magnetic stirring bar was charged with **1-Cl_2** (25 mg, 0.031 mmol), $NaBH_4$ (12 mg, 0.31 mmol), and ethanol (10 mL). The reaction was stirred at room temperature for 2 hours, then the volatiles were removed in vacuo. The product was extracted in pentane (5 x 2 mL), and isolated *in vacuo* to yield a lime-yellow residue. This compound is not stable under vacuum and therefore the pure form was not isolated for elemental analysis. ^{1}H NMR (500 MHz, C_6D_6) δ 7.96 (ddd, J = 9.8, 8.1, 1.5 Hz, 1H, CH_{Ar}), 7.79 (t, J = 8.4 Hz, 6H, CH_{Ar}), 7.56 (d, J = 7.0 Hz, 1H, CH_{Ar}), 7.09 – 6.98 (m, 11H, CH_{Ar}), 6.90 (t, J = 7.4 Hz, 1H, CH_{Ar}), 6.85 – 6.70 (m, 3H, CH_{Ar}), 1.55 (s, 9H, S$(CH_3)_3$), 0.94 (s, 9H, S$(CH_3)_3$), 0.75 (d, J = 8.4 Hz, 3H, PCH_3), -0.80 (br, 4H, Ru-BH_4), -13.04 (dd, J = 28.8, 23.4 Hz, 1H, Ru-H). ^{31}P{^{1}H} NMR (202 MHz, C_6D_6) δ 80.44 (dd, J = 24.2, 6.6 Hz, 1P, SPS), 55.93 (dd, J = 24.2, 6.7 Hz, PPh_3).

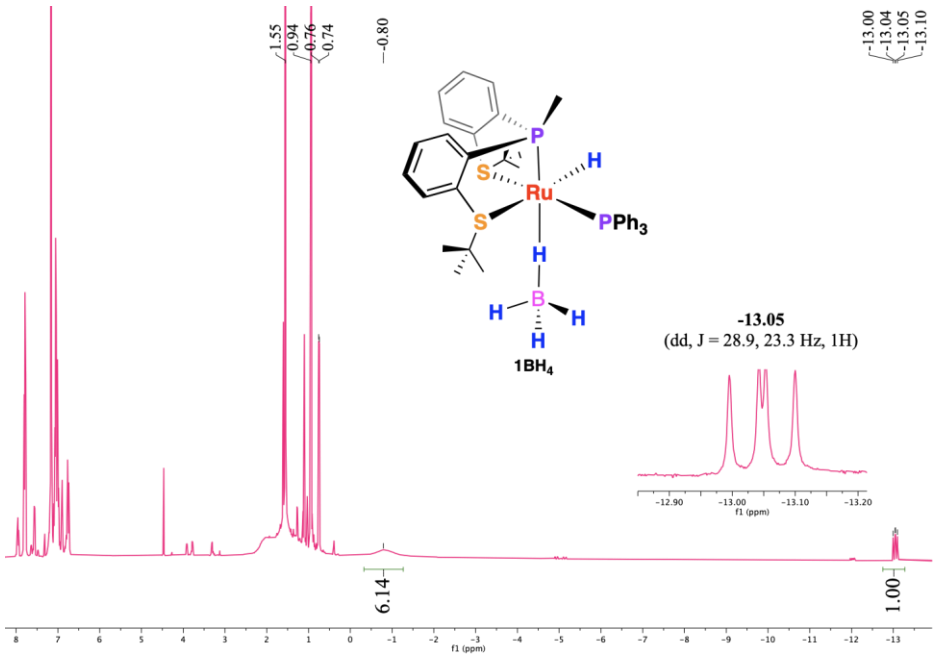

Figure S18. ^{1}H NMR (500 MHz) spectrum of borohydride **1-BH_4** in C_6D_6.

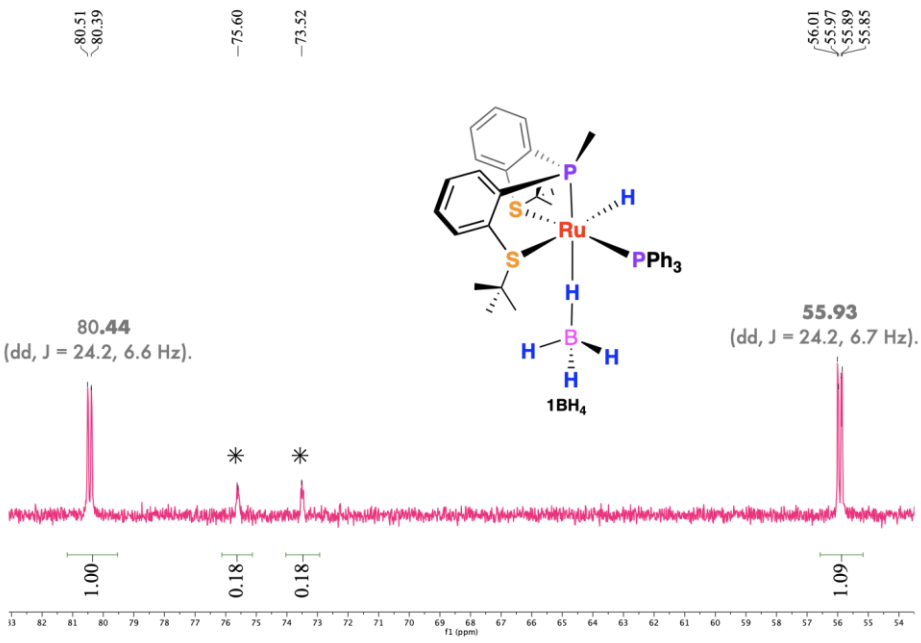

Figure S19. $^{31}P\{^{1}H\}$ NMR (202 MHz) spectrum of **1-BH4** in C_6D_6, resonances with asterisks correspond to **1-H2**.

Observation and Characterization of Ru(H)(HCO_2)(κ^3-$S^{tBu}P^{Me}S^{tBu}$)(PPh_3) (1-HCO_2). A J. Young NMR tube was charged with **1-H2** (15 mg, 0.020 mmol) in 600 μL of C_6D_6. The solution was frozen at -196 °C, degassed, and exposed to 1 atm of ^{13}C enriched carbon dioxide. The tube was warmed to ambient temperature, shaken and allowed to stand for approximately 20 minutes before starting the spectroscopic acquisition. No visible colour change was observed following carbon dioxide addition. Removal of the CO_2 atmosphere resulted in reversion to **1-H2**. ^{1}H NMR (600 MHz, C_6D_6) δ 8.91 (dd, J = 189.5, 7.7 Hz, 1H, CO_2H), 7.93 (t, J = 7.0 Hz, 6H, CH_{Ar}), 7.52 (dt, J = 6.4, 2.3 Hz, 1H, CH_{Ar}), 7.05-6.94 (m, 11H, CH_{Ar}), 6.91 (dd, J = 7.7, 2.3 Hz, 1H, CH_{Ar}), 6.85 (t, J = 7.4 Hz, 1H, CH_{Ar}), 6.76 (dd, J = 5.9, 3.2 Hz, 2H, CH_{Ar}), 6.64 (t, J = 7.6 Hz, 1H, CH_{Ar}), 1.65 (s, 9H, S$(CH_3)_3$), 1.17 (d, J = 8.4 Hz, 3H, PCH_3), 0.99 (s, 9H, S$(CH_3)_3$), -10.96 (dd, J = 27.0, 22.8 Hz, 1H, RuH). ^{13}C NMR (151 MHz, C_6D_6) δ 175.06, 168.95 (1C, CO_2H), 162.22, 148.93(d, J = 37.7 Hz), 144.56 (d, J = 44.1 Hz), 142.60 (d, J = 23.2 Hz), 139.88(d, J = 23 Hz), 136.96 (d, J = 40.7 Hz), 134.11 (d, J = 10.4 Hz), 129.73, 126.99, 124.40 (1C, CO_2), 54.13 (1C, SCCH$_3$), 53.11 (d, J = 3.4 Hz, 1C, SCCH$_3$), 30.69 (3C, SCCH_3), 28.97 (3C, SCCH_3), 15.54 (d, J = 27.1 Hz, 1C, PCH_3). $^{31}P\{^{1}H\}$ NMR (202 MHz, C_6D_6) δ 80.64 (d, J = 31.7 Hz, SPS), 60.56 (d, J = 31.4 Hz, PPh$_3$).

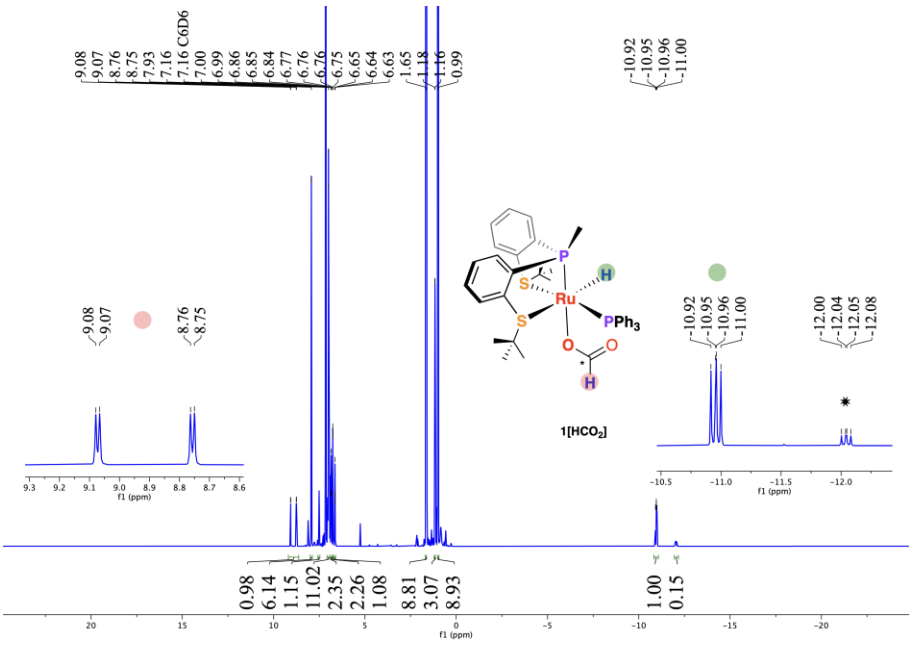

Figure S20. ^{1}H NMR (600 MHz) spectrum of $^{13}CO_2$ derived **1-HCO₂** in C_6D_6. Resonance at -12.04 corresponds to *ca* 5% of an isomer of **1-H₂** where the phosphines (from SPS ligand and PPh_3) are *trans to* each other.

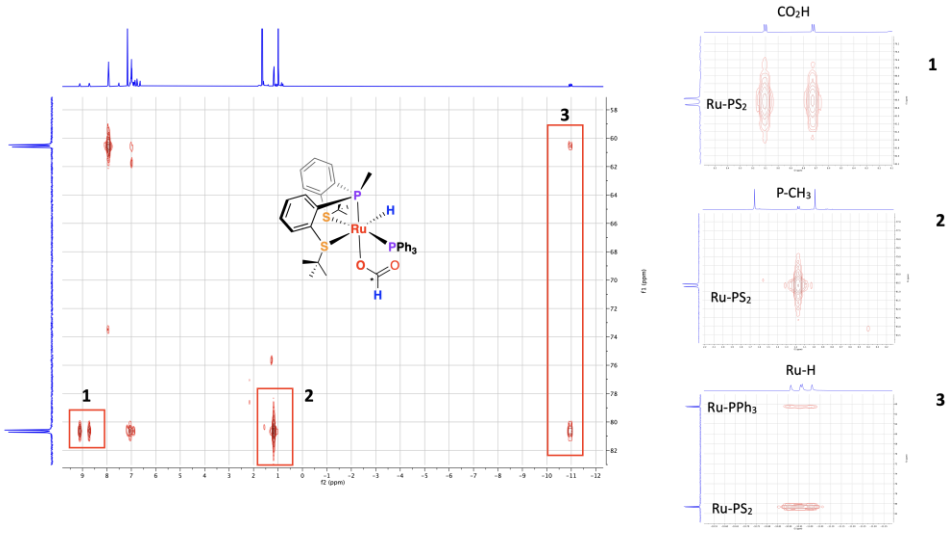

Figure S21. ^{1}H-^{31}P HMBC NMR of $^{13}CO_2$ derived **1-HCO₂** in C_6D_6 (left) and an inset (right) showing a correlation between the phosphorus atom from SPS ligand with the formate proton (**1**) and methyl substituent (**2**). A correlation between the hydride ligand and the phosphorus atoms from the SPS and PPh_3 ligands (**3**) are also observed.

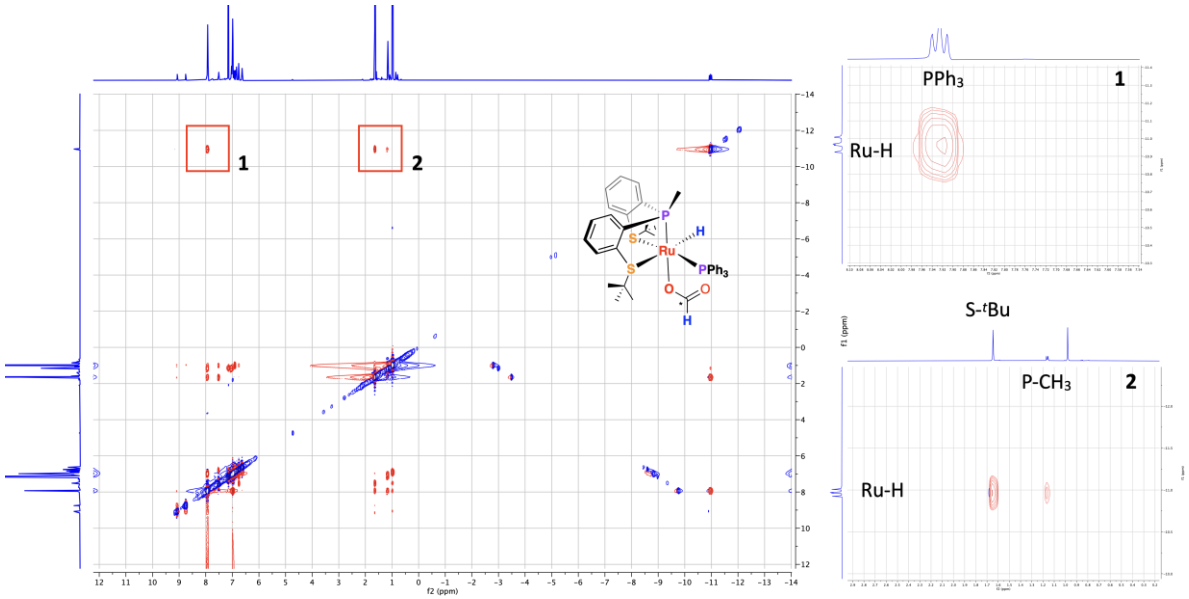

Figure S22. ^{1}H NOESY NMR of $^{13}CO_2$ derived **1-HCO₂** in C_6D_6 (left) and an inset (right) showing an NOE correlation between the hydride ligand and the aromatic protons from PPh_3 (**1**) and $P(CH_3)$ (**2**).

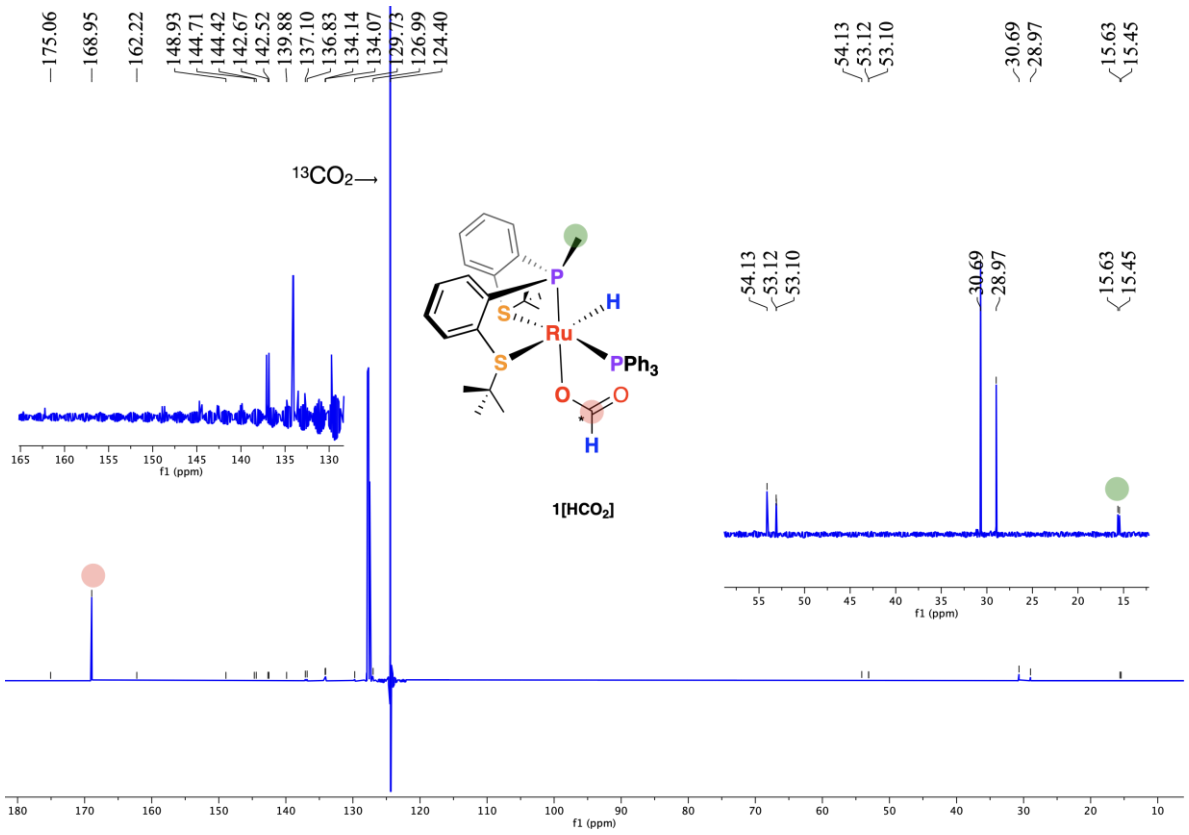

Figure S23. $^{13}C\{^{1}H\}$ NMR (151 MHz) spectrum of $^{13}CO_2$ derived **1-HCO₂** in C_6D_6.

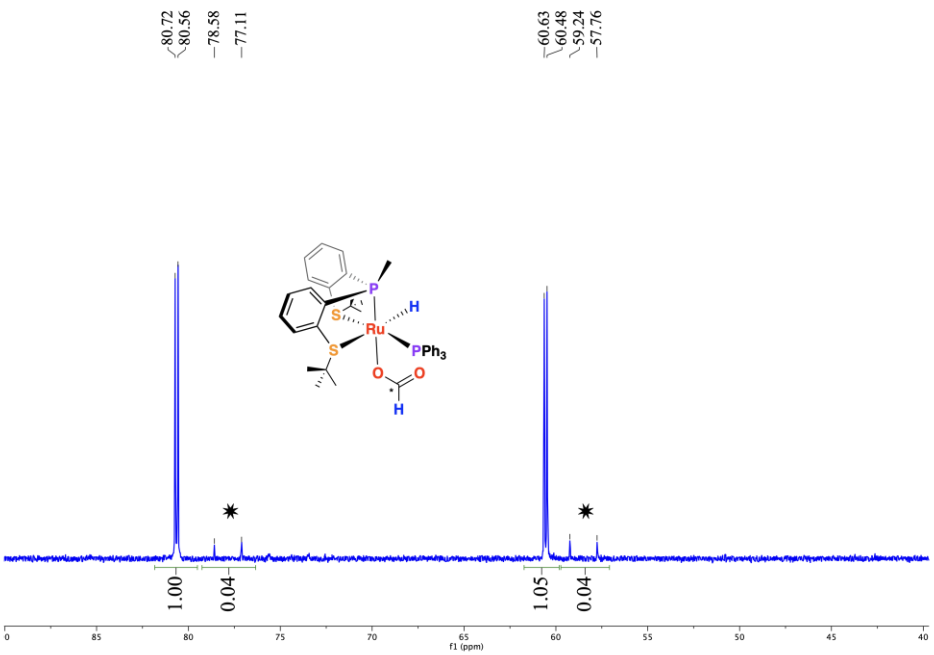

Figure S24. $^{31}P\{^{1}H\}$ NMR (202 MHz) spectrum of $^{13}CO_2$ derived **1-HCO₂** in C_6D_6. Resonances with asterisks at 77.85 (d, J = 298.8 Hz), 58.50 (d, J = 299.7 Hz) correspond to *ca* 5% of an isomer of **1-H₂** where the phosphines (from SPS ligand and PPh_3) are *trans* to each other.

A Catalytic CO_2 hydrogenation reaction with 1-H₂ was performed on an NMR scale. A J-Young NMR tube was charged with 5 mg of **1-H₂** in approximately 600 µL of THF-d_8. To this tube, 3 equivalents of $LiBF_4$ and 40 equivalents of DBU were added. The sample was frozen at -198 °C, degassed, and then exposed to 1 atm of both carbon dioxide and dihydrogen. The tube was subsequently warmed to ambient temperature and the reaction was monitored using both ^{31}P and ^{1}H NMR spectroscopy.

Upon first treating the sample of **1-H₂** with DBU/Li^+ no change was noted in the ^{1}H or ^{31}P NMR spectra, suggesting no interaction between these species and **1-H₂** (Figures S25 and S26; spectra a). However, upon the addition of CO_2 and H_2 (spectra b), peaks corresponding to the formate complex **1-HCO₂** were immediately observed, including the formate C-H resonance at δ 8.06 ppm. Simultaneously, a large signal corresponding to free formate anion ($^{-}HCO_2$) was observed was observed at δ 12.37 ppm, with an integration relative to **1-HCO₂** suggesting *ca* 18 turnovers of CO_2 hydrogenation had occurred prior to acquisition of the

NMR spectra. It should be noted that there are at least two counter cations present to balance the free formate anion, $[Li]^+$ and $[DBUH]^+$. Based on the 3:40 stoichiometry of $LiBF_4$:DBU used, we presume the downfield resonance for the formate anion is paired with $[DBUH]^+$. After the reaction had proceeded for 4 hours (spectra c), further growth in the concentration of formate anion resonance *ca* 12.75 ppm is observed, along with growth of a new signal at 8.55 ppm, which is tentatively assigned as the $[Li]^+$ salt of the formate anion. The relative intergration of the ^1H NMR formate signals is 3:1 for the $[Li]^+$: **1-HCO$_2$** species. The origin of the signal shape in the most downfield formate resonance is uncertain, but may be related to the ability of $[DBUH]^+$ to hyperconjugate multiple anions in THF or result from an overlaping N-H resonance. By 18 hours (spectra d), further changes in the NMR spectra appear to have ceased and a considerable amount of solid is present in the NMR sample.

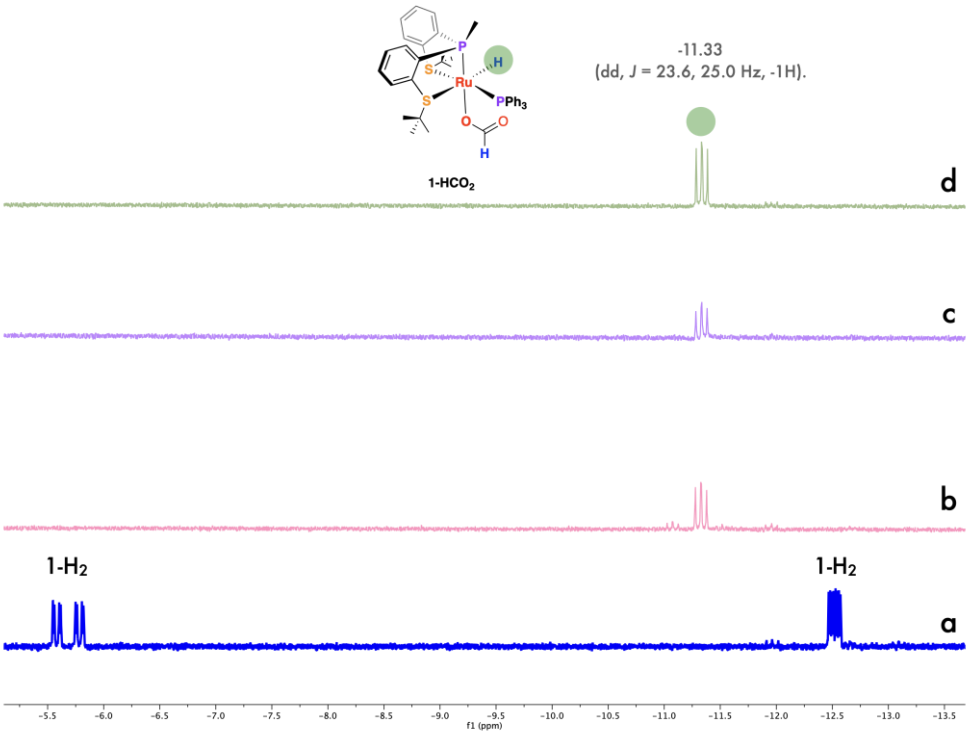

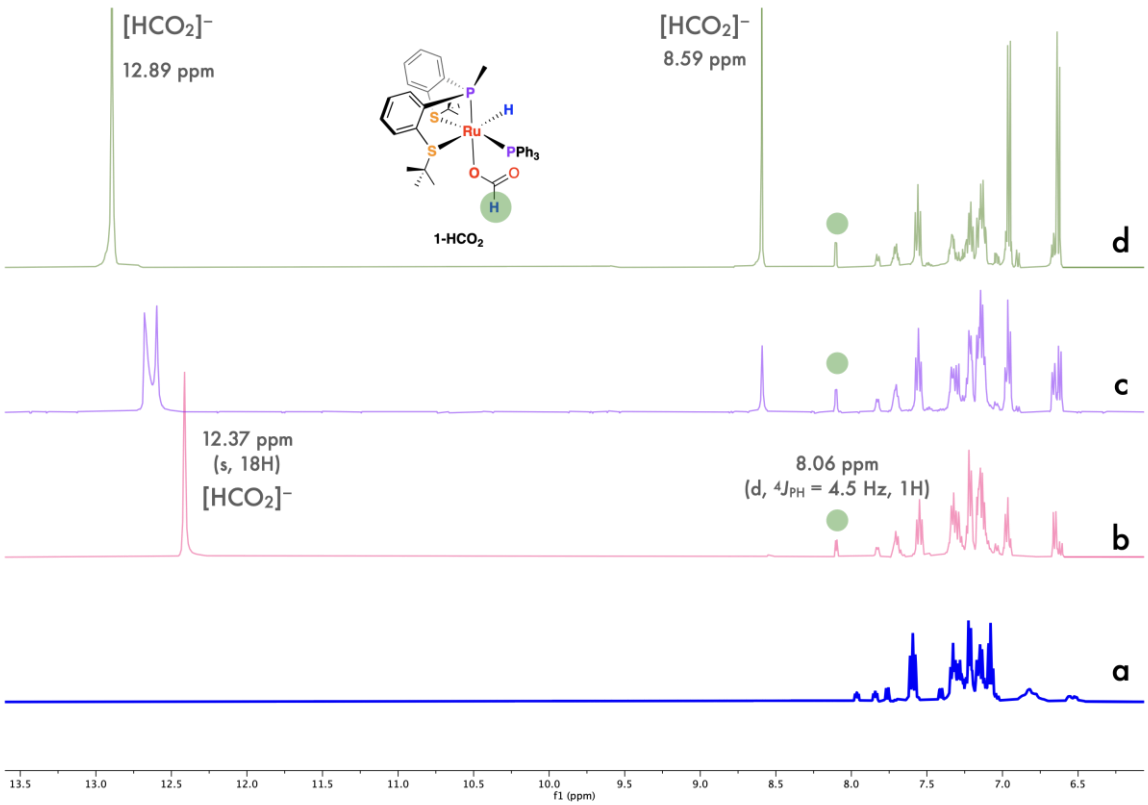

Figure S25. (a) ^{1}H NMR spectra of **1-H$_2$** in THF-d_8 after addition of 3 eq $LiBF_4$ and 40 eq DBU, (b) after addition of 1 atm CO_2 and H_2, (c) 4 h after addition of 1 atm CO_2 and H_2, (d) 18 h after addition of 1 atm CO_2 and H_2.

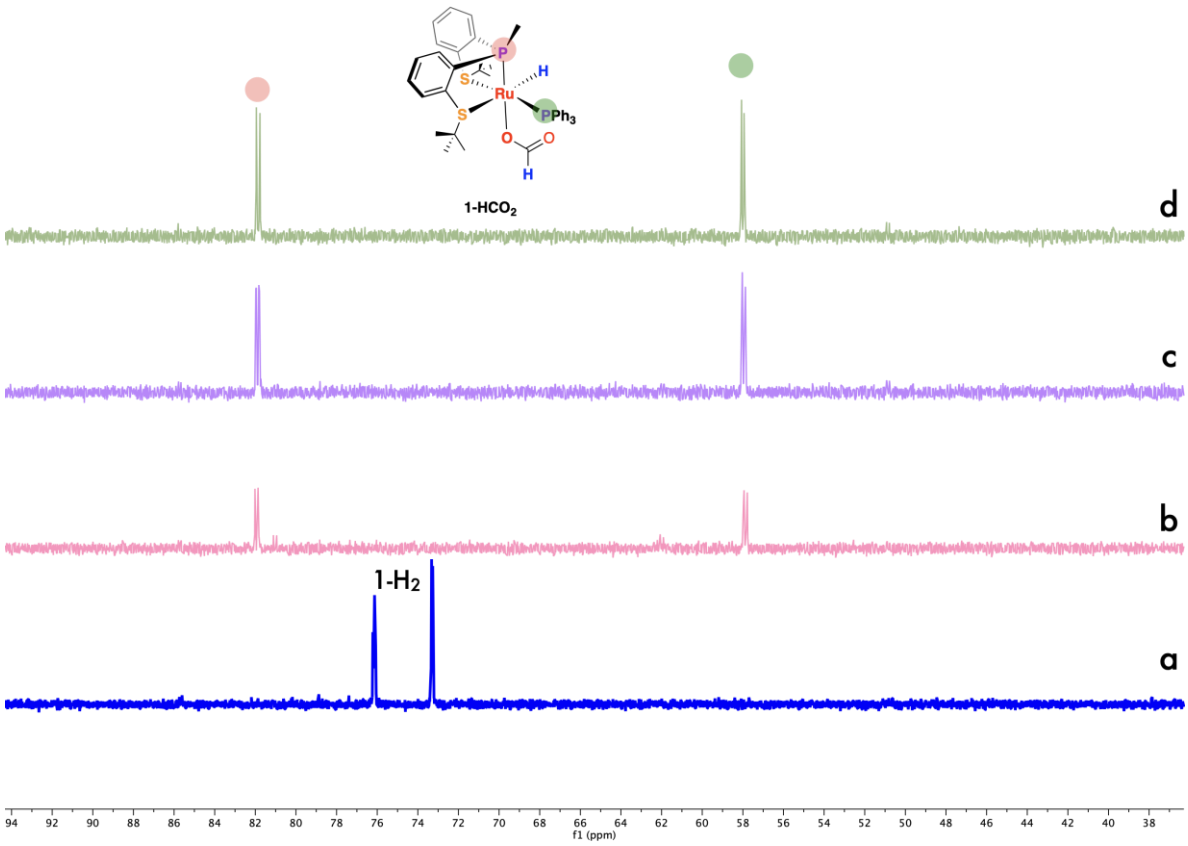

Figure S26. (a) $^{31}P\{^{1}H\}$ NMR spectra of **1-H₂** after addition of 3 eq $LiBF_4$ and 40 eq DBU, (b) after addition of 1 atm CO_2 and H_2, (c) 4 h after addition of 1 atm CO_2 and H_2 , (d) 18 h after addition of 1 atm CO_2 and H_2.

Preparation of (κ^3-SP^{Me}S)Ru(κ^2-^{tBu}SP^{Me}S)(CO) (2). The reactivity of the ^{tBu}SP^{Me}S ligand with $RuH_2(PPh_3)_3(CO)$ was initially studied in an NMR-scale reaction, targeting a CO stabilized analogue to **1-H₂**. In a glovebox, to an oven dried J-Young NMR tube was added $RuH_2(PPh_3)_3(CO)$ (48.9 mg, 0.05 mmol), ^{t}Bu^{Me}S (20.0 mg, 0.05 mmol), and 600 µL of toluene-d_8 and the sample heated at 100 °C for 24 h. The solution produced a yellow crystalline solid when stored at -42 °C overnight. Following decanting of the mother liquor and washing with cold pentane and diethyl ether, approximately 15 mg (39%) of **2** was obtained. Following characterization of **2**, an improved synthesis was established using a 2:1 ^{tBu}SP^{Me}S to Ru ratio. In a glovebox, an oven dried 100 mL Schlenk tube was charged with $RuH_2(PPh_3)_3(CO)$ (134.2 mg, 0.146 mmol), ^{tBu}SP^{Me}S (110.0 mg, 0.292 mmol), and 25 mL of toluene and heated at 100 °C 6 h. The solution was left to crystallize in a freezer at -42 °C for 12 h, and complex was isolated as a yellow solid by decanting away the mother liquor

and washing with pentane (2 x 5 mL) and diethyl ether (1 x 5 mL). After drying the solid under vacuum, 65 mg (58 %) of yellow crystalline **2** was obtained. ^{1}H NMR (600 MHz, CD_2Cl_2) δ 7.90 (t, *J* = 6.6 Hz, 1H, Ar), 7.81 – 7.70 (m, 2H, Ar), 7.65 (t, *J* = 9.2 Hz, 1H, Ar), 7.54 (t, *J* = 7.2 Hz, 1H, Ar), 7.51 (d, *J* = 6.4 Hz, 1H, Ar), 7.47 (t, *J* = 7.2 Hz, 1H, Ar), 7.36 (t, *J* = 6.9 Hz, 1H, Ar), 7.29 (t, *J* = 6.9 Hz, 1H, Ar), 7.17 (d, *J* = 7.4 Hz, 1H, Ar), 7.06 (dt, *J* = 16.9, 5.0 Hz, 2H, Ar), 6.99 (dt, *J* = 14.8, 8.2 Hz, 2H, Ar), 6.91 (t, *J* = 8.5 Hz, 2H, Ar), 2.26 (d, *J* = 8.5 Hz, 3H. P*CH₃*), 2.19 (d, *J* = 8.9 Hz, 3H, P*CH₃*), 1.62 (s, 9H, S*C(CH₃)₃*), 1.16 (s, 9H, S*C(CH₃)₃*) ^{13}C NMR (151 MHz, CD_2Cl_2) δ 199.97 (t, J = 11.07 Hz, 1C, Ru-*CO*), 160.48 (dd, *J* = 30.2, 7.2 Hz), 156.63 (dd, *J* = 29.7, 8.9 Hz, 1C, *Ar*), 143.72 (dd, *J* = 28.3, 5.7 Hz, 1C, *Ar*), 141.38 (s, 1C, *Ar*), 141.29 (s, 1C, *Ar*), 140.59 (s, 1C, *Ar*), 140.41 (d, *J* = 2.5 Hz, 1C, *Ar*), 140.29 (s, 1C, *Ar*), 140.14 (d, J = 2.6 Hz, 1C, *Ar*), 136.85 (s, 1C, *Ar*), 136.47 (s, 1C, *Ar*), 135.79 (d, *J* = 9.8 Hz, 1C, *Ar*), 134.96, (s, 1C, *Ar*), 134.69 (d, *J* = 6.2 Hz, 1C, *Ar*), 134.17 (d, *J*= 9.7 Hz, 1C, *Ar*), 130.60 (d, *J* = 2.3 Hz, 1C, *Ar*), 130.36 (d, *J* = 2.1 Hz, 1C, *Ar*), 130.12 (d, *J* = 4.4 Hz, 1C, *Ar*), 129.89 (d, *J* = 12.7 Hz, 1C, *Ar*), 129.38, (s, 1C, *Ar*), 129.32 (d, *J* = 2.3 Hz, 1C, *Ar*), 129.23 (d, *J* = 2.3 Hz, 1C, *Ar*), 129.04 (d, *J* = 2.8 Hz, 1C, *Ar*), 128.76 (d, *J* = 13.5 Hz, 1C, *Ar*), 128.58 (d, *J* = 2.7 Hz, 1C, *Ar*), 126.30 (d, *J* = 6.8 Hz, 1C, *Ar*), 121.64 (d, *J* = 6.5 Hz, 1C, *Ar*), 54.27 (s, 1C, *C*$(CH_3)_3$), 49.37 (s, 1C, *C*$(CH_3)_3$), 32.38 (s, 3C, C*(CH₃)₃*), 30.20 (s, 3C, C*(CH₃)₃*), 15.51 (d, *J* = 29.2 Hz, 1C, P*(CH₃)*), 13.30 (dd, J = 27.3, 3.4 Hz, 1C, P*(CH₃)*). ^{31}P{^{1}H} NMR (202 MHz, CD_2Cl_2) δ 61.80 (d, *J* = 298.9 Hz, 1P), 44.16 (d, *J* = 299.8 Hz, 1P). IR (KBr): 1950 cm^{-1} (Ru-CO).

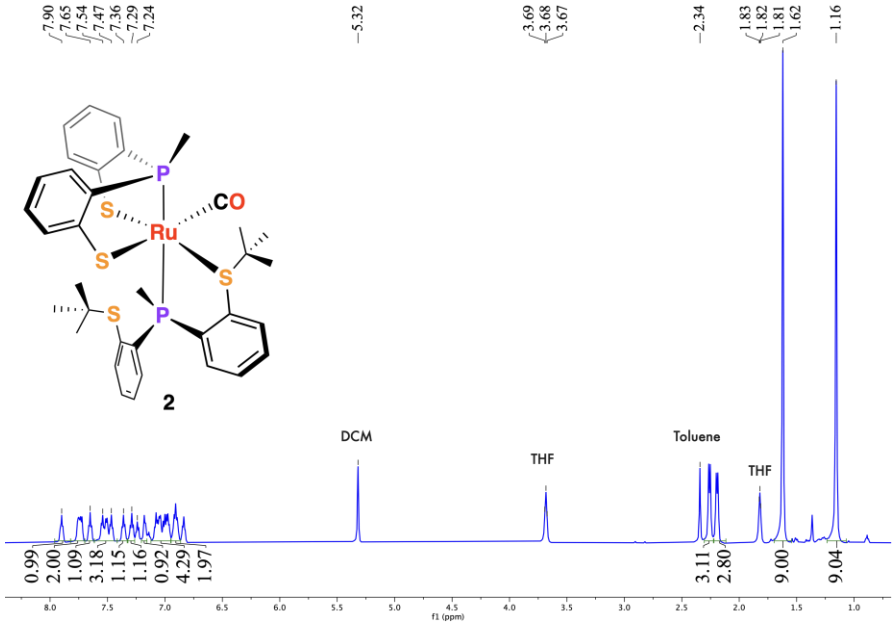

Figure S27. ^{1}H NMR (500 MHz) spectrum of **2** in CD_2Cl_2.

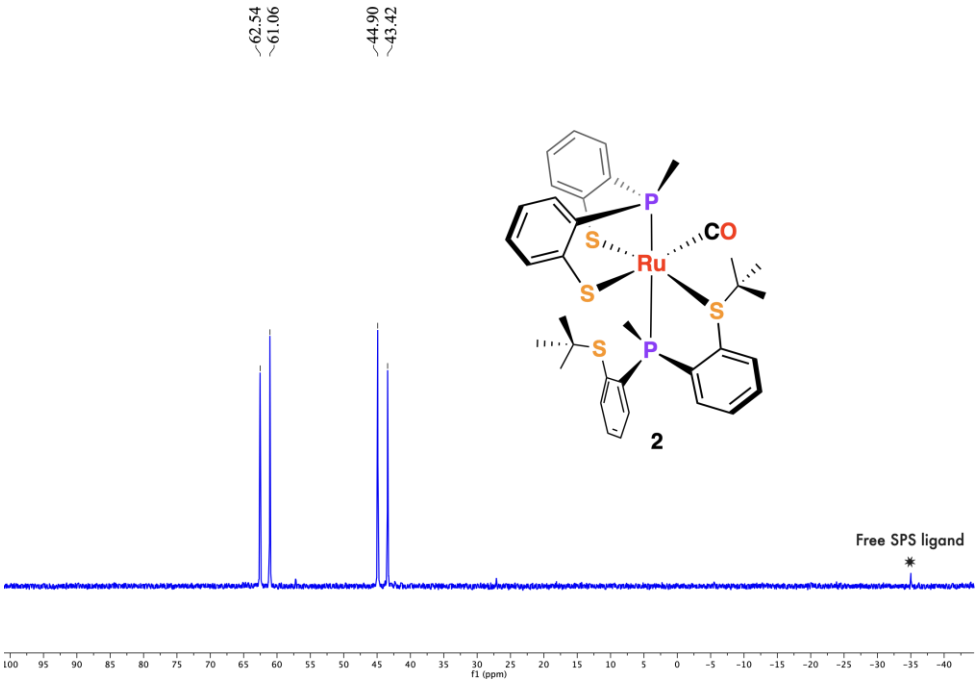

Figure S28. ^{31}P{^{1}H} NMR (202 MHz) spectrum of **2** in CD_2Cl_2.

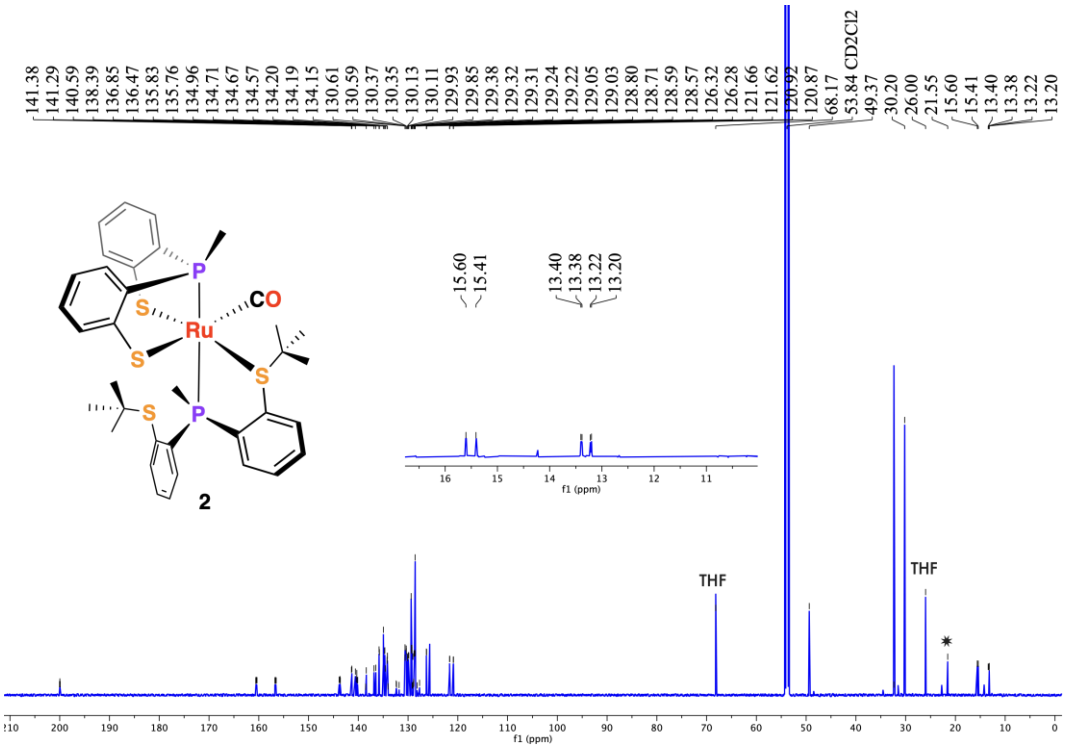

Figure S29. $^{13}C\{^{1}H\}$ NMR (126 MHz) spectrum of **2** in CD_2Cl_2.

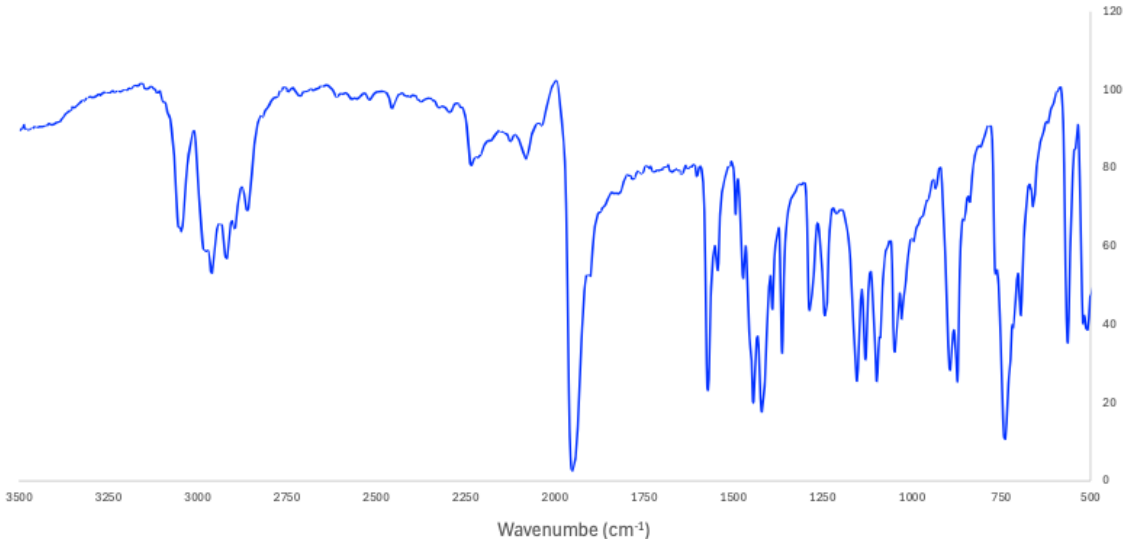

Figure S30. Solid-state IR spectrum of **2** in KBr.

Details of Catalytic Reactions

General Procedure for Catalytic Hydrogenation of CO_2 to Formate.

In a glovebox, a 50 mL glass reactor liner was charged with a catalyst stock solution in THF (approximately 3 mM, 0.3 μmol catalyst), LiOTf (if used as an additive, 230 mg, 1.5 mmol), DBU (2.34 g, 15 mmol), and 8 mL of THF. The reactor liner was then placed into a 50 mL Parr reactor, which was sealed, removed from the glovebox and pressurized sequentially with 250 psi of CO_2 followed by 250 psi of H_2 through a Y-valve inlet at ambient temperature. The reactor was subsequently heated to 80 °C and mechanically stirred for the desired reaction time. The reaction was terminated by removing the heat source, cooling the reactor in an ice-water bath, and venting the vessel. The reaction solution, which typically contained suspended colorless solid, was then transferred to a 100 mL round-bottom flask, using THF to transfer any solid products. All volatiles were removed under reduced pressure. The colorless solid was dissolved in D_2O, and DMF was added as an internal standard (typically 100 to 400 μL of standard) and the formate product quantified by ^{1}H NMR spectroscopy, with a one second delay between scans. Catalytic trials were performed in at least triplicate, and the standard deviation between trials are reported as the uncertainty value in turnover number (TON).

Table S1. Control Experiments for CO_2 Hydrogenation to Formate.[a]

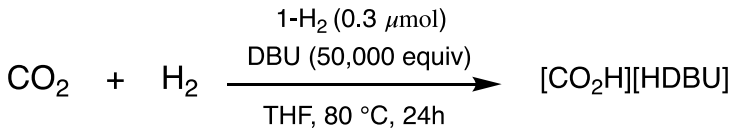

Entry	[Ru]	TON[b]	Yield[c] %
1	**1-H$_2$**	30200 (200)	60
2	**2**	3000 (200)	6
3	$[Ru(PPh_3)_3]Cl_2$	1500 (200)	3
4	Blank	N/A	~2[d]

[a]Reaction conditions: 250 psi of CO_2/250 psi of H_2, **1-H$_2$** (0.3 μmol), DBU (2.34 g, 15.0 mmol), THF (8 mL), 80 °C. [b]TONs were quantified using ^{1}H NMR spectroscopy; reported values are the average of three trials with the standard deviation in parentheses. [c]The yield based on DBU. [d]1.5 mmol of LiOTf and no ruthenium source was added.

Table S2. Catalytic Trials of CO_2 Hydrogenation to Formate to Test Homogeneity of Active Species.[a]

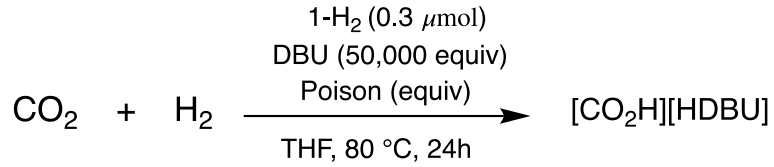

Entry	Additive	TON[b]	%
1	No Additive	30200 (200)	60
2	$^{t\text{Bu}}SP^{\text{Me}}S$ (10 eq)	32000 (500)	64
3	Mercury	33900 (800)	68
4	PMe_3 (2 eq)	19000 (1000)	38

[a]Reaction conditions: 250 psi of CO_2/250 psi of H_2, **1-H₂** (0.3 μmol), DBU (2.34 g, 15.0 mmol), THF (8 mL), 80 °C. TONs were quantified using ^{1}H NMR spectroscopy; reported values are the average of three trials with the standard deviation in parentheses. [b]This number is the observed TON after 24 h.

A series of experiments outlined in Table S2 were conducted to probe the homogeneity of the active catalytic species. Entry 2 indicates that addition of excess SPS ligand does not reduce the catalytic productivity of the reaction, inconsistent with a potential loss of pincer ligand toward formation of a particulate Ru active species. Likewise, the Hg drop test in entry 3 exhibits no loss in reaction yield, consistent with a homogenous active species. Finally, addition of a near stoichiometric quantity of strong donor ligand PMe_3 (entry 4) results in only proportional loss of catalytic performance. In the event of a nanoparticle based active catalyst, as significant inhibition would be expected from stoichiometric (or even sub-stoichiometric) poisoning given the limited ratio of active surface to inactive interior metal atoms in most nanoparticle catalysts.

General Procedure for Catalytic N-Formylation of Amines.

In an example procedure, a 50 mL glass reactor liner in a glovebox was charged with a **1-H₂** stock solution in THF (approximately 10 mM, 4 μmol catalyst), pyrrolidine (142.2 mg, 2 mmol, s/c= 500), and THF (8 mL). The reactor liner was then placed into a 50 mL Parr reactor, which was sealed, removed from the glovebox, pressurized to 500 psi with CO_2, and

finally charged with 500 psi of H_2 gas through a Y-valve inlet at ambient temperature. The vessel was heated to 120 °C and mechanically stirred for the specified period. The reaction was terminated by removing the heat source, cooling the reactor in an ice-water bath, and the residual gases were released carefully in a hood. The yield of N-formyl pyrrolidine and residual pyrrolidine were determined by GC using p-xylene (308 μL) as the internal standard.

Table S3. N-formylation of amines with H_2 and CO_2 catalyzed by 1-H_2.[a, b]

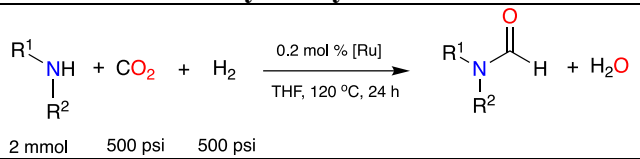

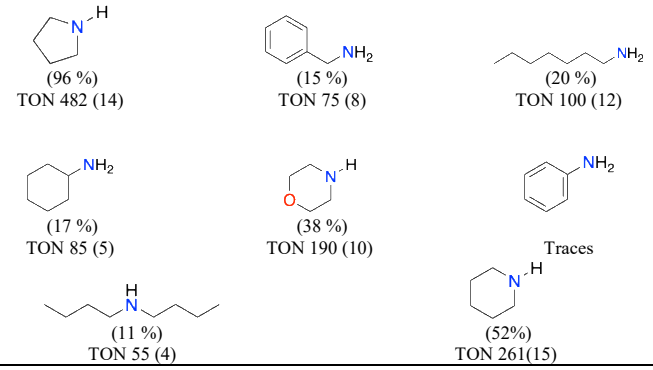

[a]Reaction conditions: 500 psi of CO_2/500 psi of H_2, **1-H_2** (4 μmol), amine (2.0 mmol), THF (10 mL), 120 °C, 24 h. [b]Yields based on the amount of formamide production as determined by GC/FID. Reported values are the average of two or more trials.

Table S4. Selected crystallographic data for complexes 1-Cl_2, 1-H_2, and 2.

	1-Cl_2	1-H_2	2
Empirical Formula	$C_{39}H_{44}Cl_2P_2RuS_2$	$C_{39}H_{46}P_2RuS_2$	$C_{35}H_{40}OP_2RuS_4$
Formula weight [g/mol]	810.82	741.93	767.96
T [K]	173 (2)	173 (2)	173 (2)
Wavelength (Å)	0.71073	0.71073	0.71073
Z	8	8	4
Crystal system	Monoclinic	Monoclinic	Orthorhombic
Space group	C2/c	P21/n	Pna*21*
a [Å]	38.8520(4)	10.0461(3)	17.6021(9)
b [Å]	14.8412(15)	25.5274(8)	12.8281(7)
c [Å]	18.3680(18)	17.2498(6)	17.2940(9)
α [°]	90°	90°	90°
β [°]	90.004(3)°	97.0994(12)	90°
γ [°]	90°	90°	90°
Volume [$Å^3$]	10591.2(18)	4389.8(2)	3905.0(4)
Density (calculated)	1.017 g/cm^3	1.434 g/cm^3	1.521 g/cm^3
Absorption coefficient	0.556 mm^{-1}	0.547 mm^{-1}	0.722 mm^{-1}
Crystal size [mm^3]	0.45 x 0.04 x 0.02	0.430 x 0.220 x 0.06	0.16 x 0.16 x 0.11
Reflections collected	95136	14656	10977
R(reflections)	0.0660 (5803)	0.0487 (11708)	0.0368 (9927)

Single crystal X-ray diffraction data was collected on a Bruker D8 Venture diffractometer equipped with a Photon II CMOS area detector using Mo-Kα radiation from a microfocus source (Bruker AXS, Madison, WI, USA). Crystals were cooled to the collection temperatures under streams of cold N_2 gas using a Cryostream 800 cryostat (Oxford Cryosystems, Oxford, UK). Hemispheres of unique data were collected using strategies of scans about the omega and phi axes with 0.5° frame widths. The Bruker Apex4 software suite was used for unit cell determination, data collection, data reduction, absorption correction and scaling, and space group determination.[3]

The structures of **1-H_2** and **2** were solved by direct methods as implemented in SHELXS.[4] The structure of **1-Cl_2** was solved by an iterative dual space method as implemented in SHELXT.[5]

[3] Apex4, AXScale, and SAINT, version 2022.1, Bruker AXS, Inc., Madison, WI, 2022.
[4] G. M. Sheldrick, SHELXS, v.2013-1, 2013.
[5] G. M. Sheldrick, *Acta Cryst. Sect. A: Found. Adv.* 2015, **71**, 3-8.

Crystal structures were refined by full matrix least squares refinement against F^2 using SHELXL v. 2019.[6] Olex2 was used a graphical interface for structure visualization and model building.[7] Non-hydrogen atoms were located from the difference map and refined anisotropically. Hydrogen atoms bonded to carbon were placed in calculated positions and constrained to ride on the carrier atoms. The hydride ligands in **1-H$_2$** were located from the difference map and their coordinates freely refined; the positions to which they converged correspond to the expected vertices of an octahedral Ru coordination polyhedron. All hydrogen atom thermal parameters were constrained to ride on the carrier atoms. In all three refinements, difference map peaks corresponding to disordered molecules of solvation were observed which could not be reliably modeled. The contribution of this disordered matter was estimated and corrected for using PLATON SQUEEZE.[8] Compound **2** crystallized in the acentric space group *Pna*2$_1$ and was refined as an inversion twin with a minor domain volume fraction of 4.6%.

The diffraction data for **1-Cl$_2$** was truncated during integration to 0.94 Å. The signal to noise at this resolution shell is 6.53, but R_{int} is 38% and climbs sharply at higher angles. This suggests that the signal to noise is being artificially increased due to overlap of scattering from multiple domains, and removal of this data prevents systematic errors from being introduced into the refinement. Restraints for rigid bond behavior were applied to carbon atom thermal parameters for **1-Cl$_2$** which compensates for the reduced data-to-parameters ratio.[9] The reliability of the refinement of **1-Cl$_2$** is supported by its agreement to the isostructural hydride.

[6] G. M. Sheldrick, *Acta Cryst. Sect. C: Struct. Chem.* 2015, **71**, 3-8.
[7] O. V. Dolomanov, L. J. Bourhis, R. J. Gildea, J. A. K. Howard and H. Pushman, *J. Appl. Cryst.* 2009, **42**, 339-341.
[8] A. Thorn, B. Dittrich and G. M. Sheldrick, *Acta Cryst. Sect. A.: Found. Adv.* 2012, **68**, 448-451.
[9] A. L. Spek, *Acta Cryst. Sec. C: Struct. Chem.* 2015, **71**, 9-18.